

Expertise and confidence explain how social influence evolves along intellectual tasks

Omid Askarisichani^{a,*}, Elizabeth Y. Huang^{b,c}, Kekoa S. Sato^a, Noah E. Friedkin^{c,d}, Francesco Bullo^{b,c}, and Ambuj K. Singh^a

^aDepartment of Computer Science, University of California, Santa Barbara, CA 93106; ^bDepartment of Mechanical Engineering, University of California, Santa Barbara, CA 93106; ^cCenter for Control, Dynamical Systems and Computation, University of California, Santa Barbara, CA 93106; ^dDepartment of Sociology, University of California, Santa Barbara, CA 93106

This manuscript was compiled on November 17, 2020

Discovering the antecedents of individuals' influence in collaborative environments is an important, practical, and challenging problem. In this paper, we study interpersonal influence in small groups of individuals who collectively execute a sequence of intellectual tasks. We observe that along an issue sequence with feedback, individuals with higher expertise and social confidence are accorded higher interpersonal influence. We also observe that low-performing individuals tend to underestimate their high-performing teammate's expertise. Based on these observations, we introduce three hypotheses and present empirical and theoretical support for their validity. We report empirical evidence on longstanding theories of transactive memory systems, social comparison, and confidence heuristics on the origins of social influence. We propose a cognitive dynamical model inspired by these theories to describe the process by which individuals adjust interpersonal influences over time. We demonstrate the model's accuracy in predicting individuals' influence and provide analytical results on its asymptotic behavior for the case with identically performing individuals. Lastly, we propose a novel approach using deep neural networks on a pre-trained text embedding model for predicting the influence of individuals. Using message contents, message times, and individual correctness collected during tasks, we are able to accurately predict individuals' self-reported influence over time. Extensive experiments verify the accuracy of the proposed models compared to baselines such as structural balance and reflected appraisal model. While the neural networks model is the most accurate, the dynamical model is the most interpretable for influence prediction.

influence systems | appraisal networks | performance | human subject experiment | opinion dynamics | balance theory | data mining | convex optimization | deep learning | quantitative sociology | transactive memory systems | social comparison theory | confidence heuristic | nonlinear dynamics

Inevitably, relationships among collaborating actors evolve over time, with people changing their opinions or appraisals of one another. Such relationships form a network structure called an influence/appraisal network (1–6) with signed edges that may portray trust/distrust, friendship/enmity, and like/dislike (7). In our study, we use the terms *influence* and *appraisal* interchangeably. Investigations of the evolution of such networks draw on a rich body of literature on opinion dynamics. DeGroot *et al.* (8), and Friedkin *et al.* (2) propose widely-established models of opinion change and the conditions of consensus formation. Altafini *et al.* (9)'s model considers diverging opinions under antagonistic interactions. Such models are surveyed in Proskurnikov *et al.* (10). Influence system specifications play a pivotal role in all of these studies. Note that these opinion dynamic models assume the influence network of a group is given a prior. Our goal is

to quantitatively estimate the influence network among individuals in a group, where the influence network within the group is represented by a row-stochastic matrix. The estimation of this matrix paves the way for solving problems such as influence maximization (11, 12); viral marketing (13, 14); personalized recommendation (15); feed rankings (16); target advertisement (17); selecting influential tweeters (18, 19); and selecting informative blogs (20).

Classic studies of the antecedents of interpersonal influence include French and Raven's work (21) on the bases of social power, and cognitive biases research (22) showed that individuals are accorded influence based on their job titles, past performance, friends' opinions, etc. There has also been mathematical modeling of the endogenous evolution of appraisal networks. Friedkin *et al.* (23) showed how reflected appraisal mechanisms elevate or dampen the self-weights of group members along a sequence of issues. Jia *et al.* (5) proposed the DeGroot-Friedkin model, where the appraisal network evolves as a function of the social power within the group. Jia *et al.* (24) also studied how over time, the coevolution of appraisal and influence networks leads to a generalized model of structural balance theory (25–30). Mei *et al.* (31) modeled collective learning in teams of individuals using appraisal networks, where the appraisal dynamics change as a function of the performance of individuals within the team.

Research on transactive memory systems (TMS) (32–35) provide an approach to formation of influence systems. A

Significance Statement

How do individuals become influential within a team and to what extent is influence affected by cognitive biases and heuristics? Predicting social influence has important applications in finance, politics, and any task-oriented teams. We propose machine learning models to predict interpersonal influence in teams using message content, communication times, and individual task performance. We also propose an intuitive cognitive model that tests and validates the hypotheses that expertise, confidence, and psychological cognitive biases drive the formation of social influence. Our findings on groups of human subjects show the proposed models significantly improve the prediction of influence networks compared to baseline algorithms.

O.A., K.S.S., and E.Y.H. analyzed the data. E.Y.H. developed the dynamic model and O.A. developed the machine learning models. O.A. and E.Y.H. performed the statistical tests. N.E.F., F.B., and A.K.S. actively participated in the discussion and gave critical comments. All authors substantially contributed to the design of the research and the writing of the paper.

The authors declare no conflicts of interest.

²To whom correspondence should be addressed. E-mail: omid55@cs.ucsb.edu

TMS is characterized by individuals' skills and knowledge, combined with members' collective understanding of which members possess what knowledge (34, 36, 37). As members observe the task performances of each other, their understanding of "who knows what" tends to converge to an accurate assessment, leading to greater coordination and integration of members' skills. Empirical research (32–35) across a range of team types and settings demonstrate a strong positive relationship between the development of a team TMS and team performance. The research indicates for the purpose of improving self performance, individuals tend to find experts via demonstrability in their group during intellectual tasks (38, 39). Unlike judgemental issues, for intellectual tasks there exists a demonstrable mathematical or verbal correct answer that can be distinguished by high-performing teammates (38).

Research in social comparison theory has shown that individuals tend to evaluate their own abilities by biased comparisons with their peers. In particular, Woods (40) describes several motivations behind biased social comparison such as self-esteem protection (41), lack of appropriate incentives (42), or the existence of dominant individuals who skew member contributions (43, 44). Davison *et al.* (44)'s experimental results show that low-performing individuals tend to overestimate (resp. underestimate) low-performers (resp. high-performers), i.e. high-performing individuals are better able to recognize other experts than low-performing individuals. To study such psychological cognitive biases, several scientists have conducted group experimental studies by self and peer evaluations (43, 45, 46).

Research on confidence heuristics (47, 48) has shown that the more self-confident individuals are, the more influence they are accorded by others. London *et al.* (49) find that "the single significant behavioral difference between persuaders and persuadees was in the expression of confidence". Confidence heuristics is defined based on a social and psychological norm, whereby more confidently expressed arguments signal better information, allowing an efficient revelation of information and decision-making based on expressed confidence (47).

We build on the above three lines of research. Although the problem of estimating social power (5, 50), and influence networks have been studied before (51–53), existing research lacks empirical studies as they are mostly based on theory and grounded on simulation-based analyses (31). Moreover, previous studies on influence estimation has focused on proxies of influence such as propagation of hashtags, quotes, and retweets (53–58). An impactful study by Almaatouq *et al.* (59) finds that social influence is significantly correlated with confidence and correctness. However, no estimation method is proposed that mathematically formulates how these factors contribute to the underlying dynamics of influence. Furthermore, we find these two factors alone do not lead to the most accurate predictions of self-reported influence for small teams with static networks in this empirical setting. Studies on the empirical estimation of the weighted network of who-influences-whom are rare (60, 61). In the present work, we probe more deeply into the foundations of the links between individual performance, self-confidence and social comparison on interpersonal influence. Our work bridges the gap between empirical and simulation-based results by utilizing sociology-inspired mechanisms and machine-learning based models to estimate the social influence in groups. Overall, to the best of our

knowledge, this study is the first to estimate the influence matrices in a text-based shared media among individuals, collected from a human subject experiment, where teammates communicate via a broadcast system to solve intellectual tasks.

Our contributions in this paper are threefold. First, we find empirical support for widely established theories in psychology, sociology and management regarding the effect of TMS (32, 33, 35), confidence heuristics (47, 48) and social comparison theory (40, 44) on individuals' influence over their teammates. Second, we introduce a novel cognitive dynamical model based on the aforementioned theory regarding how influence is accorded from others. This cognitive model is validated against the empirical data and can be used to estimate influence matrices using past reported influence matrices and individual performance. We provide analytical and simulation results on the asymptotic behavior of the model for the case with identically performing individuals. Third, we propose a machine learning-based model for estimating influence networks using any features such as individual performance, past influence matrices, and communication contents as well as communication timestamps. Extensive experiments show that our proposed neural network model surpasses all baseline algorithms with statistical significance on multiple merits.

Experimental Design

We collected data for 31 teams comprising of four human members each. Each team is presented with the same sequence of 45 trivia questions that fall into three categories: Science and Technology, History and Mythology, and Literature and Media. Every team has two minutes to answer each question. First, team members answer individually before the answers are revealed to the team. Second, they are asked to collaborate on a single unanimous response. Lastly, the platform reveals the correct answer immediately after a team submits their answer. Thus, they are provided with immediate feedback on their performance after every response. The design also incorporates a multi-part incentive for subjects to seek the correct answer on each question: an evolving team performance score; an option to consult with one of four available AI-agents after the team discussion (the AI-agents may or may not provide a correct answer) which, if exercised, must lower the team's performance score regardless of whether provides a correct or incorrect answer; and feedback to each team on correct and incorrect answers. This multi-part incentive structure operated to concentrate the attention of the team on the evaluation of the relative expertise of their members.

This experimental setting was run on the Platform for Online Group Studies (POGS) and tests the participants' intellectual memory. Each experiment consists of nine rounds of five intellectual questions each, with teams surveyed after each round. At the end of each round, subjects are asked to record the influence of their teammates in their decision-making process as a percent value, such that the sum of all values adds up to 100. Every subject assumes they are given a total of 100 chips and instructed to distribute these chips to indicate the relative importance of each member in determining their own final answer on all past problems. Thus, the number of chips that a subject allocates to a particular member should indicate the extent to which they were personally influenced by that member. The number of chips that subjects allocate to themselves should indicate the extent to which their final

answer was not affected by the conversation. If an individual felt that all conversations so far provided no influence to their choice of answer, then they would put 100 besides their own name. If the conversation caused them to abandon their approach to the problem, then they are instructed to put zero beside their own name and allocate all the chips to one or more of the other members.

After normalization, the self-reported interpersonal influences form a row-stochastic influence matrix for every round, containing only non-negative entries (in a row-stochastic matrix every row sums up to one). The platform ensures that in each inquiry, the reported influence matrix has non-negative entries and is row-stochastic. Additionally, the platform collects a log of all the instant messages including time of message and content during every question, the individual and group answers, and the self-reported influence matrices.

Since the platform displays the correct answer to every question immediately after the group submits its response, attentive subjects can use the individual responses and text discussion to keep track of which individual teammates may have expertise in one or more areas over the course of the experiment. Thus, along the problem sequence, the team may solve problems more efficiently and also more accurately.

Results

The experimental logs show that most teams reached a consensus when answering the questions. Every team reached a consensus on average 42 times on the sequence of 45 questions posed to them. All self-reported influence networks are found to be unilaterally connected and the majority are strongly connected. More precisely, out of 279 influence matrices reports, only six ($\sim 2\%$) are not strongly connected which happen only when one person assigns all their influence to only themselves. Almost all of the not strongly connected cases were reported early in the experiment. With respect to the convergence of influence, in the last round, in 90% of the teams, at least half of the subjects reported the same ranking order of influences for all members including themselves. Additionally, we observe that in $\sim 74\%$ of the teams the influence assignments converge to a single person as being the most influential unanimously reported by the team, and that $\sim 23\%$ of the teams converge to two individuals as being equally the most influential members.

Origins of interpersonal influence. The following hypotheses, motivated from past research, are empirically supported by our experimental results:

Hypothesis 1. *Individuals with higher expertise are accorded higher interpersonal influence from the group.*

Hypothesis 2. *Individuals with lower expertise have diminished ability to recognize experts in the group.*

Hypothesis 3. *Individuals with higher confidence are accorded higher interpersonal influence from the group.*

In this experiment, subjects read and answer every question individually. Ergo, the individual performance (expertise) can be measured by the ratio of correct answers one gives individually, prior to seeing others' answers and the discussion phase. Assuming individuals can potentially keep track of others' expertise by recalling their answers or their chat messages, we study if individual expertise plays a prominent role in the

amount of social influence one receives. Note that M shows the ground truth influence matrix.

Qualitatively, we can look at the dynamics of every subject's appraisal of every subject over time. For example, Fig. 1 show a team of four subjects and $M_{ij}^{(t)}$ shows the amount of influence subject i assigns to subject j in every round. It is clear that on aggregate and over time the individuals found member #2 to be the most accurate and therefore they reported member #2 to be the most influential person. Also, we know after answering all questions, member #2 was more accurate than anybody else (cumulative correctness rate for member #1= 49%, member #2= 70%, member #3= 36%, and member #4= 58%). This is an example of the emergence of the first hypothesis. This figure illustrates how the interpersonal appraisal reflects the underlying expertise and how teammates were able to uncover that expertise early on in the experiment.

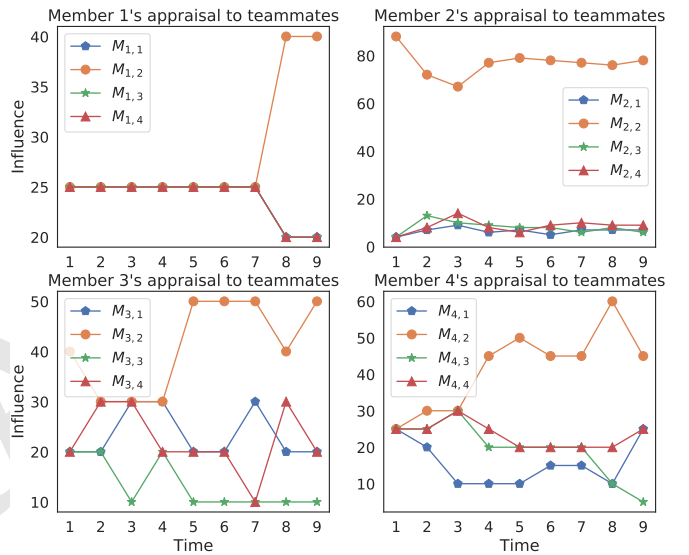


Fig. 1. Dynamics of the influence matrix in one team: M shows a 4×4 influence matrix for this team. Every panel shows how much every subject reports others influenced them over time. In other words, it shows the amount of appraisal every person assigns to team members including themselves over time. After answering all questions, we observe that member 2 is the most accurate (cumulative correctness rate for member #1= 49%, member #2= 70%, member #3= 36%, and member #4= 58%). This figure illustrates the team's interpersonal appraisals reflect the accuracy of the team members, which was ascertained early on in the experiment.

To quantitatively test the three hypotheses, we define few terms based on the influence matrix: confidence, persuasiveness, and mean reversion. The individual perception (local) definition of social confidence and persuasiveness for person i take into account column i of the influence matrix. However, the team perception (global) definition uses the stationary probability for person i (index i of the left dominant eigenvector of the influence matrix). The stationary distribution, also known in the literature as the eigenvector centrality (62), takes into account the connectivity level in the network for infinite length paths and hence provides a more general point of view. Note that $v_L(X)$ represents the stationary distribution for row-stochastic matrix X , $\mathbb{1}_n$ represents n -dimensional column vector of ones, and $\text{diag}(x)$ represents a matrix with diagonal entries of vector x and zero everywhere else.

Confidence is provided in Eq. [1]. The local definition for persuasiveness is Eq. [2], and the global definitions for persua-

siveness is given in Eq. [3]. To compute the persuasiveness we consider the reflective relative appraisal matrix C , which is defined by removing the diagonal elements from matrix M and re-scaling to be row-stochastic. Another term defined in the following is expertise which is the proportion of questions every member individually answers correctly.

- *Expertise*: Individual correct answer rate (individual accuracy or individual performance) — the proportion of questions one has individually answered correctly up to any given time ($\frac{\#\text{correct answers}}{\#\text{answers}}$).
- *Confidence*: Self-appraisal — the amount of influence one assigns to oneself at any given time.

$$M_{ii}^{(t)}. \quad [1]$$

- *Persuasiveness*: Appraisal by others — the amount of influence everybody else is assigning to a particular team member at any given time.

The local perception (accumulative):

$$\frac{1}{n-1} \sum_{j, j \neq i} M_{ji}^{(t)}. \quad [2]$$

The global perception (eigenvector):

$$(v_L(C^{(t)}))_i, \quad [3]$$

where $C^{(t)} = \text{diag}((M^{(t)} - D^{(t)})\mathbf{1}_n)^{-1}(M^{(t)} - D^{(t)})$ shows relative interpersonal influence matrix at round t where $D^{(t)}$ is a diagonal matrix with the diagonal entries of influence matrix $M^{(t)}$ at round t .

- *Mean reversion*: Reversion to the mean (uniformity) in the appraisals that an individual holds of their teammates:

$$D_i = \sum_{j=1}^n \|M_{ij} - \frac{1}{n}\|_2^2, \quad [4]$$

For the sake of abbreviation, throughout this study, we use the aforementioned terms. The empirical distribution of the expertise shows that individuals are more accurate than a random guess (on average individuals have about 50% correct rate when the expected value is 25% for four-choice questions). Also, we find controlling for the difficulty of the questions does not change the cumulative correctness rate distribution.

The empirical distribution of confidence and persuasiveness shows that *on average* people tend to assign influence uniformly to their teammates, including themselves. This means that for our experiments on groups of four, a matrix with 0.25 in every element can be a competitive baseline for estimating influence matrices. Also, the distributions show that individuals tend to give greater influence to themselves than to others. Moreover, as we observe the empirical distributions for both local and global perceptions are similar in this dataset, we use them interchangeably.

Correlation study of interpersonal influence. To study the relationship between expertise and persuasiveness, we compute the correlation between the amount of persuasiveness with expertise after answering all questions. We use the final influence matrix reported by every team and their expertise at the end of the experiment. Note that, this data satisfies correlation, regression, and causation studies' requirements since the amount of influence one reports for themselves, other teammates report

about that person, and their individual correct answer rate are independent and identically distributed. We report empirical evidence for all the aforementioned hypotheses. Pearson correlation results show that there is a statistically positive correlation between expertise and persuasiveness (r -value = 0.35 and p -value $< 2e - 4$) (see Supplementary Fig. S2). This is the statistical evidence for Hypothesis 1. This phenomenon was predicted by cognitive science and evolutionary anthropology studies depicting individuals naturally engage in selective social learning (59, 63, 64). This finding is also an empirical result for the seminal research in the theory of TMS (33–35). We provide an empirical evidence for Hypothesis 2 via predicting mean reversion (Eq. [4]) using expertise in the following subsection. Finally, we also find that there is a statistical positive correlation between persuasiveness and confidence (r -value = 0.22 and p -value $< 2e - 2$). This is the statistical evidence for Hypothesis 3. This result is consistent with reported empirical findings (59, 65, 66). Becker *et al.* (65) and Almaatouq *et al.* (59) both measure confidence as proportionate to the change in the individual answer before and after the discussion (so-called "weight on self") and present evidence for its correlation with one's popularity. This is also aligned with past research in confidence heuristics (47, 48, 67–69). These two significant correlation were replicated in a different empirical experiment on wisdom of crowds where the network structure was dynamic (59). However, in this experiment, the result is surprising since individuals communicate only through chat and nonetheless the expertise and the self-confidence impacted people's judgment stronger than any cognitive biases. Also, our experiments show the type of definition for persuasiveness does not change the sign of this relationship, nor its statistical significance. Thus, due to the large correlation between global and local perceptions of persuasiveness, the similarity of their distributions, and more straightforward local definition, we use its local definition in the rest of the paper.

Regression study of interpersonal influence. Although the correlation between pairs of variables provides a simple view of their relationship, we can utilize a regression model to not only take into account multiple variables but also their interactions. This would incontrovertibly draw a more robust and general picture of the aforementioned metrics. Hence, here we intend to estimate one's average influence reported by their teammates at the end of the experiment. We use the Generalized Linear Model (GLM) method to solve the regression problem. Table 2 shows the coefficients and their statistical significance in three least-squares problems (each column shows a separate test).

The empirical evidence for Hypothesis 2 is obtained via regression on expertise and mean reversion. Table 1 shows the regression results for predicting mean reversion for every individual. Our results show the more expert one individual is, the more different than equal they appraise their teammates as the expertise is positively and statistically significant of predictive power of the reversion to the mean (p -value < 0.05) in all teams. It also shows this is an individual feature as the team average performance is not statistically significant while individual performance stays statistically significant. In fact, this result is the motivation behind using expertise as a weighted average in the cognitive dynamical model described in the next section.

Table 1. Regression result for predicting mean reversion: The statistical significance demonstrated in regards of p -value: * $p < 0.01$, ** $p < 0.05$. This result shows the individual performance (expertise) statistically and positively is of predictive of mean reversion.**

Predicting Mean reversion	Feature-set 1	Feature-set 2
Intercept	0.10 ***	0.10 ***
Individual performance	0.07 **	0.08 ** (VIF: 1.21)
Team performance		-0.004 (VIF: 1.21)
	Log-likelihood: 384.4 AIC: -764.8 BIC: -754.4	Log-likelihood: 384.4 AIC: -762.8 BIC: -747.2

Table 2 shows that introducing more variables in columns has increased log-likelihood, Bayesian Information Criterion (BIC), and Akaike Information Criterion (AIC). It shows that expertise has a consistently positive and statistical predictive-power on persuasiveness (the empirical evidence for Hypothesis 1). The statistical significance is robust even after adding many more variables shown in the rightmost column. Also, confidence has a positive statistical predictive-power to predict persuasiveness (the empirical evidence for Hypothesis 3). However, its coefficient (importance) is less than the expertise (aligned with research in confidence heuristics (47)). This result is found when the platform provides immediate feedback for every question. If no feedback is provided or there is no right or wrong answer (i.e. judgmental questions), people might use confidence as a more substantial metric in their appraisal distribution.

Causality study of interpersonal influence. To study the order of the effects by confidence, persuasiveness, and expertise and to what extent their effect is supported by data, we propose to use a forecasting causality test. We use Granger causality — a statistical concept of causality that is based on prediction (71–73). To study the causality of the aforementioned variables, we compute expertise, confidence, and persuasiveness in every round. Thus, in this data, for every person, we have three time series with nine data points. For every person, we compute Granger causality of these time series and study what percentage of change in individuals’ expertise, confidence, and persuasiveness have statistical causal effects. Note that the exact number of lags, which were statistically significant, could uncover the precedence of these variables. That plausibly opens the door to studying the order of different effects, such as hypotheses 1 and 2, leading to social influence.

Applying statistical tests on three time series per individual is pregnant with false discovery and is absolutely crucial to adjust our results. Ergo, in the following results, obtained p -values are adjusted using Benjamini-Hochberg (BH) (74) controlling procedure with false discovery rate (FDR) of 5%.

Fig. 2 depicts empirical evidence for Hypothesis 1 and 3. Fig. 2 shows multiple Granger causality tests on the effect of confidence, persuasiveness, and expertise on one another. These results are obtained after applying the BH procedure with FDR=5% that has required p -value < 0.03 as a statistical significance threshold. Even though the time series are relatively short (only nine data points), this result shows that in most individuals there is statistical causation from confidence to persuasiveness and vice versa over time. The results also show there is a causal relationship from expertise to confidence (aligned with confidence heuristics) and also persuasiveness

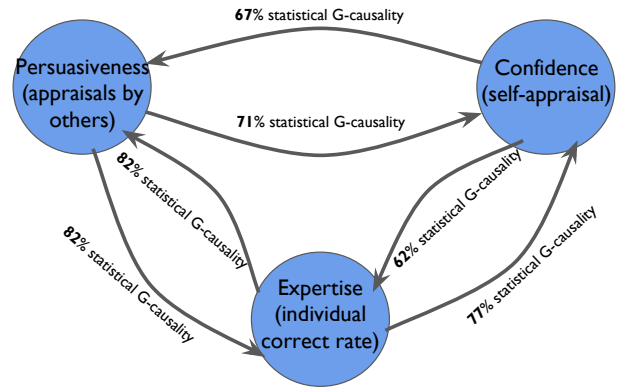


Fig. 2. Granger causality result: This figure shows the proportion of statistically significant Granger causality of timeseries of confidence, persuasiveness and expertise in all teams. The p -values have been corrected using Benjamini-Hochberg (BH) procedure with False Discovery Rate of 5% has required p -value < 0.03 as statistical significance threshold.

(TMS (33)). Note that unlike the correlation experiment that was taking into account only the final influence report and expertise, these results are computed from time series of influence and performance for every individual during the course of the experiment.

To study the order of effects given in Fig. 2, we use the proportion of statistically significant Granger causality associated with different lags. Every lag depicts five questions, as we inquire about their influence matrix every five questions. In this regard, we test the causality once using lag=1 and then by using lag=2. We analyze the proportion of statistical significance only with lag=1 and the rest that needs at least two previous time data points (lag=2). Thus, we sort the effects based on the descending order of the proportion of lag=1 as an estimate for the underlying order. From the effects in Fig. 2, Expertise \rightarrow Confidence seems to be the fastest (as it has the most number of statistical significance effects with lag=1 compared to the rest of the effects). Afterward, Confidence \rightarrow Persuasiveness and Expertise \rightarrow Persuasiveness both come very close to each other. And at last, Persuasiveness \rightarrow Confidence seems the slowest among all. In other words, the order shows that the expertise of individuals quickly impacts their confidence. Both their confidence and their expertise then lead to persuasiveness. However, it seems that confidence has a slightly faster effect. This is perfectly aligned with the past research in confidence heuristic (47) and means that people have an immediate effect by social power and confidence, indeed faster than expertise. However, still, after some time (two lags in this experiment) expertise as a heuristic would be more prominent in the amount of persuasiveness (as 70% of individuals have this causal relationship after maximum two lags). In the end, persuasiveness can also lead to confidence; however, although it happens very often, it happens slower than the aforementioned effects. The delay of the persuasiveness affecting confidences could be because the platform shares individuals’ answers with everyone but does not disclose their appraisals of each other. Therefore individuals must learn their confidence from persuasiveness through multiple discussions.

Influence matrix estimation. Studying the problem of estimating the influence matrix is novel and challenging. Our data

Table 2. Regression result for predicting persuasiveness: Generalized Linear Model (GLM) regression coefficients and their statistical significance in estimating local persuasiveness at the end of the experiment (after answering 45 questions). Statistical significance is portrayed with * for $p < 0.01$ for ** and $p < 0.05$. The amount of Variance Inflation Factor (VIF) is provided in parenthesis; this factor estimates how much the variance of a regression coefficient is inflated due to multicollinearity in the model. It is known (70) that statistical results remain significant in models with multicorrelated independent variables when $VIF < 5$. Evidently, the findings are robust. Taking into account the interactions of all variables, we find that expertise and confidence are consistently statistically predictive of persuasiveness. Networks are extracted from the time and the content of chat messages among individuals and defined in the "Feature-set from logs" part.**

Predicting Persuasiveness	Feature-set 1	Feature-set 2	Feature-set 3	Feature-set 4
Intercept	0.13 ***	0.19 ***	0.12 ***	0.12 ***
Expertise	0.20 ***		0.17 *** (VIF: 1.05)	0.17 *** (VIF: 1.11)
Confidence		0.14 ***	0.11 *** (VIF: 1.05)	0.12 *** (VIF: 1.06)
Response network out-degree				0.00 (VIF: 2.63)
Sentiment network out-degree				0.002 ** (VIF: 2.54)
	Log-likelihood: 162.86 AIC: -321.7 BIC: -316.3	Log-likelihood: 162.90 AIC: -321.8 BIC: -316.4	Log-likelihood: 168.12 AIC: -330.2 BIC: -322.1	Log-likelihood: 170.18 AIC: -330.4 BIC: -316.8

present an unprecedented opportunity to understand team behavior and estimate the interpersonal influence system of teammates. Even though this is a large set of states to estimate, there are a few constraints that make this task feasible. The matrix is row-stochastic, and all elements fall into $[0, 1]$. Note that M represents the ground truth influence matrix, and \hat{M} represents the estimated influence matrix.

Influence matrix estimation is an applicable problem. Estimating individuals' influence directly from their communication logs and individual performances are useful in any team-based organization. Studying the longitudinal dynamics of a team influence system is rife with information about team behavior. In this experiment, the estimation method is applied for every team in every round using a history of influence matrices, text embeddings, and estimated expertise before that round. Using explainable machine learning and dynamical models, we also attempt toward uncovering the underlying predictive power of different features and mechanisms leading to higher interpersonal influence in teams.

Before studying models to estimate influence matrices, we need a set of measures (metrics) to gauge the accuracy of the estimated influence matrices with the ground truth ones. We use two classical metrics: Mean Square Error (MSE) and the Kullback-Liebler (KL) divergence. Together they portray two different measures of accuracy. MSE pays more attention to the exact estimation of each number in the matrix while KL divergence on each row of the influence matrix focuses on the similarity of the distributions.

The MSE and KL divergence of two row-stochastic matrices M and \hat{M} with n rows are defined as follows,

$$\text{MSE}(M, \hat{M}) = \frac{1}{n} \|M - \hat{M}\|_F^2 = \frac{1}{n} \sum_{i=1}^n \sum_{j=1}^n |M_{ij} - \hat{M}_{ij}|^2, \quad [5]$$

$$\text{KL}(M, \hat{M}) = \frac{1}{n} \sum_{i=1}^n \left(\sum_{j=1}^n M_{ij} \log \frac{M_{ij}}{\hat{M}_{ij}} \right). \quad [6]$$

Depending on the application, one may choose any of these metrics. To showcase the generality of our proposed models, we present results on both metrics (Fig. 5).

We propose three models with a spectrum of explainability:

- (i) A black-box deep learning model which is the most accurate,
- (ii) A white-box linear model using convex optimization that explains substantial features leading to interpersonal influence (Table 3),
- (iii) A cognitive dynamical model which postulates an underlying mechanism. This dynamical model unlike the

other two machine learning models does not require much training data as it only has one scalar hyperparameter to choose from. In the following, we introduce the results of estimation using these models.

Influence matrix estimation: cognitive dynamical models. We propose discrete-time dynamical models, of the form $\hat{M}^{(t+1)} = T(\hat{M}^{(t)}, x^{(t)})$, that are formulated such that established sociological concepts are baked into their equations. These non-machine learning models only take the history of past local influence weight information and individuals' performance values. These models can be used to provide a single or multi-round forecast of the influence matrices for successive rounds of the experiment.

Our results compare the accuracy of various dynamical models, which are described below in the Materials and Methods section. The models are a baseline model, model based on Hypothesis 1, model based on Hypotheses 1 and 2, and model based on Hypotheses 1, 2 and 3. The models assume that individuals can observe each other's expertise, which they take into account when readjusting the influence weights assigned to one another.

We consider single-round and multi-round forecast, to compare how the models perform when using the previous round's influence matrix versus only the initial round's influence matrix.

The *single-round forecast* predicts the influence matrix at future rounds $t + 1 \geq 2$ using the reported influence matrix from the previous round $M^{(t)}$ and the expertise $y^{(t)}$. Note that for the single-round forecast, the prediction comes from the following modification to the dynamics, $\hat{M}^{(t+1)} = T(M^{(t)}, y^{(t)})$. Fig. 3 (left) illustrates the error of a given model.

The *multi-round forecast* predicts $\hat{M}^{(t)}$, for any future round $t + 1 \geq 2$, using the initial reported influence matrix $M^{(1)}$ and the previous round's expertise values $y^{(t)}$ as inputs. The following details how the dynamical models are modified to give multi-round forecasts. To estimate $\hat{M}^{(2)}$, the map $T(M^{(1)}, y^{(1)})$ is used. For subsequent rounds $t \geq 3$, the estimate comes from $\hat{M}^{(t+1)} = T(\hat{M}^{(t)}, y^{(t)})$. In summary, the ground truth influence matrix data is propagated over a sequence of rounds to predict the influence matrix at future rounds. Fig. 3 (right) illustrates the error of a given model.

Overall for the single and multi-round forecast, we observe increased estimation accuracy for the models that capture more hypotheses. For the single-round forecast, we observe

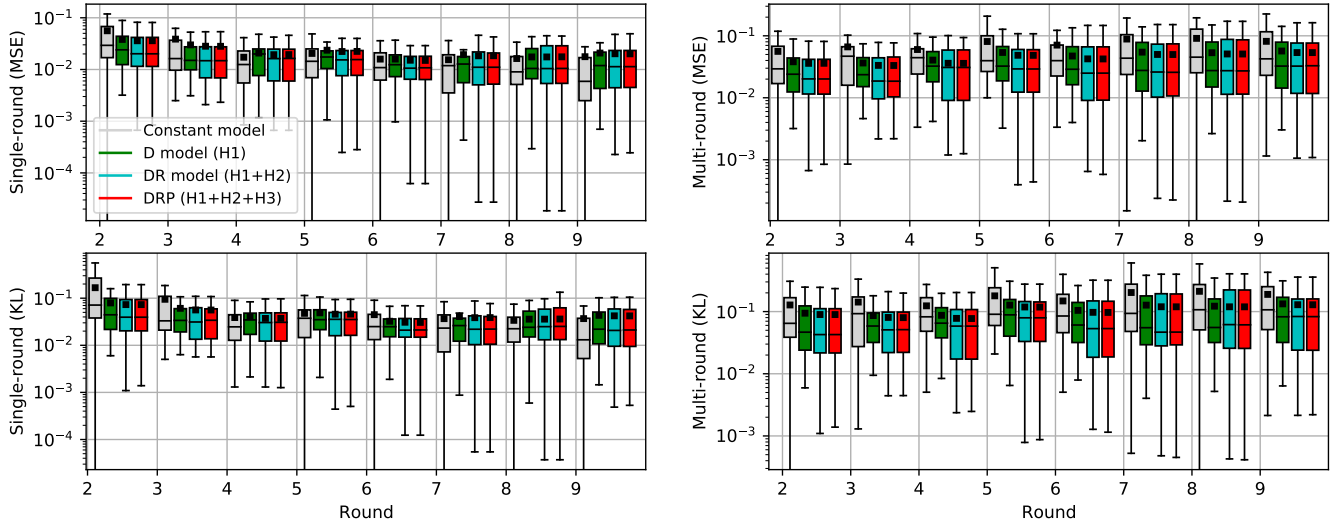


Fig. 3. Cognitive model evaluation: The mean squared error (MSE) and the Kullback-Leibler (KL) divergence for different dynamical models over nine rounds of influence matrix estimation. Differentiation (D model) takes into account hypothesis 1. Differentiation, Reversion (DR model) is inspired by hypotheses 1 and 2. Differentiation, Reversion, Perceived (DRP model) uses hypotheses 1, 2, and 3. For the models, we use the hyperparameter $\tau = 0.4$. In this figure boxes show the interquartile range of the errors, the whiskers show minimum and maximum of the range of the distribution. In each box, the dot shows the average and the line shows the median of the portrayed distribution. **Left:** Single-round forecast error of various dynamical models for predicting the influence matrix one round ahead. The models estimate $\hat{M}^{(t+1)}$ using the expertise $\bar{y}^{(t)}$ and the reported influence matrix from the previous round $M^{(t)}$. **Right:** Multi-round forecast error of various dynamical models for predicting the influence matrix multiple rounds ahead. Outliers are not shown for better readability. The models estimate $\hat{M}^{(t+1)}$ using the expertise $\bar{y}^{(t)}$ and the initial ground truth $M^{(1)}$ influence matrix reported by individuals. For rounds $t + 1 \geq 2$, the dynamics use the predicted influence matrix from the previous round $\hat{M}^{(t)}$, instead of $M^{(t)}$. For rounds $t \geq 4$, the influence network remains relatively constant, so the cognitive dynamical model offers incremental improvements to the baseline models for single-round forecast. However, this model gives significant improvements in accuracy from baseline models for all rounds in multi-round prediction.

that the accuracy increases for later rounds since individuals adjust influence weights less as the experiment goes on. However, the accuracy for later rounds does not give significant improvements compared to the constant baseline model, since the influence weights remain relatively constant for rounds $t \geq 4$. For the multi-round forecast, as expected, we see that the accuracy decreases for predictions of later rounds; yet consistently provides the most accurate predictions of the influence matrices regardless of whether the model is given the most up-to-date ground truth values. In the following, we also show that the cognitive dynamical model gives competitive predictions compared to the machine learning models.

Influence matrix estimation: machine learning models. We introduce machine learning models to predict the influence matrix at every round. These powerful models are able to take multiple features extracted from the logs of the experiment and learn a mapping to estimate the corresponding influence matrix. In order to learn such mappings, they require training data. Thus, we use a portion of collected logs as the training and apply the trained model on the unseen logs.

In order to predict the influence matrix at round t , we use time and content of text messages from the broadcast communication logs until round t , individual correct percent until round t , and reported influence matrices before round t in the following.

- **Connectivity networks:** In broadcast communication logs, the time between two messages can reveal a directed and weighted evolving network structure among teammates. This approach implies a basic assumption: if a message B appears on a chat log close enough in time to an earlier sent message A, then B is likely a response to A; and, the larger the time gap

between two messages is, the less likely the later message is a response to the earlier message. For a message m occurring at time $m.time$ on the log, we define the set of its responses and the connectivity networks as follows

$$R(m) = \{r \mid m.time < r.time \wedge t_1 \leq r.time - m.time \leq t_2 \wedge r.sender \neq m.sender\}$$

$$A_{ij} = \sum_{\substack{p.sender=i \\ q.sender=j \\ q \in R(p)}} weight(p, q), \quad [7]$$

We define the weights in the connectivity networks (given in Eq. [7]) in three different ways. First is Response network in which the weights in the network, similar to Amelkin *et al.* (75), are calculated based on the duration a response as $weight(p, q) = e^{-\gamma|p.time - q.time|}$. This networks represents the responsiveness of every individuals toward every other member. The likelihood of a message being a response degrades with the increase of the time gap between the two messages. Second is Sentiment network in which we use Valence Aware Dictionary and sEntiment Reasoner (VADER) as the sentiment analysis toolbox (76) on words in the response message as $weight(p, q) = sentiment(q)$. Third is the Emotion network in which Affective norms for English words (ANEW) are used as the emotion analysis toolbox (77) that examines arousal, valence, and dominance of words in the response message. The weight for emotion network is computed as $weight(p, q) = emotion(q)$. In all networks, the summation is performed over all suitable pairs (p, q) of messages p and q in a team's chat log. Thus, these networks are represented as a $n \times n$ matrix with float values and no self-loop.

- **Message content embeddings:** We use natural language processing to analyze the content of messages. The text em-

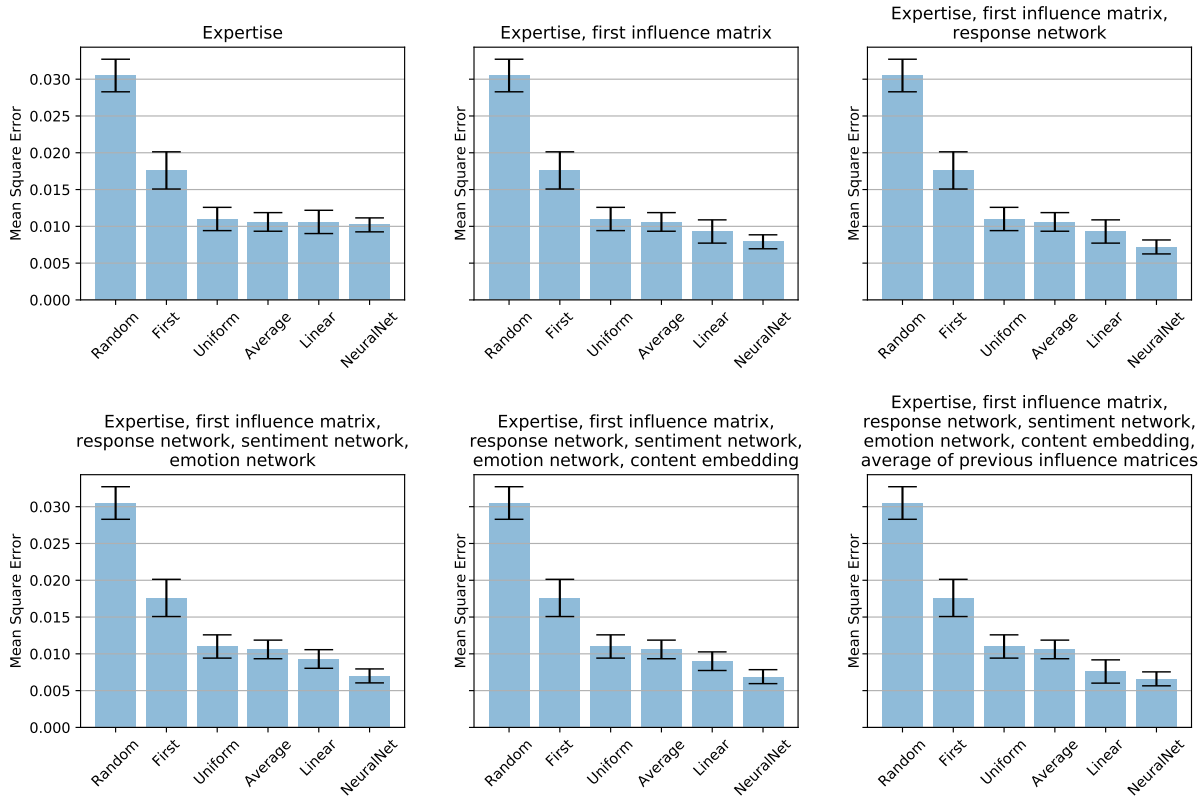


Fig. 4. Improvement in machine learning models by adding more features: Average of Mean Square Error (MSE) of estimated influence matrix from the ground truth in the test set of influence matrices. Titles show the list of features fed to the models. The error bar shows the standard deviation in 1000 bootstrap on test error. Both machine learning models improve when given more features from the logs.

beddings for sentences (78) are generated from a pre-trained sentence embedding model by the last layer of the encoder in the state-of-the-art model, a Robustly Optimized BERT Pretraining Approach (RoBERTa) (79, 80), is generated.

- History of influence matrix: Previous influence matrices.

- Expertise: Individual cumulative correctness rate.

We propose a linear maximum likelihood estimation model using convex optimization and a deep neural network model. Fig. 6 shows the architecture of the neural network model (see Methods and Materials). They both similarly intend to find a linear or nonlinear combination of the aforementioned input features to estimate a row-stochastic influence matrix. We compare the proposed models to the baseline models with a variation of different input features. All models are trained with 80% of the data and tested on the withheld 20%. To compute the statistical significance, we draw 1000 bootstraps with replacement from the hold-out test set.

Due to the application, for every round, we can assume we only have access to the first influence matrix, and we need to predict all influence matrices in future rounds with that. Hence, in Fig. 4, we use only the first influence matrix with expertise, text embeddings, and so forth, in every round, to predict a 4×4 influence matrix. It shows the average of Mean Square Error (MSE) for the estimated influence matrix from the ground truth influence matrix (reported by individuals) in every round for every team. MSE is defined by Eq. [5]. Fig. 4 depicts linear and neural network-based models consistently surpass other baselines with any sets of features. Also, it

shows the proposed models are powerful as the more features are introduced, the more accurate they can get.

In another setting, for every round, we assume we have access to the previous influence matrix and expertise to predict the current influence matrix. For this setting, there are more baselines that we can compare our proposed models against. Fig. 5 (left) shows MSE divergence error for models using previous influence matrix and expertise. Similarly, the neural network-based model surpasses all baselines and provides statistically significant lower MSE. It is worth mentioning that proposed linear model (Eq. [13]) is competitive with the proposed neural network model (Fig. 6). Also, interestingly, the proposed cognitive dynamical model (Eq. [12]) which does not require any training and is described by a mechanism that postulates past research in social psychology works significantly better than other baselines and competitively close to the proposed machine learning models. Note that both machine learning models use optimization methods for training that requires several steps to converge.

Fig. 5 shows MSE and KL divergence of the estimated influence matrix from the ground truth reported by individuals. MSE is defined on two matrices in Eq. [5] and KL divergence in Eq. [6]. MSE and KL divergence provide two different perspectives regarding the efficacy of influence estimation. MSE formulation emphasizes the exact values in matrices, while KL divergence attends to the discrete probability distribution in corresponding rows of two matrices. Fig. 5 shows that for both error measurements, the two proposed models work efficiently

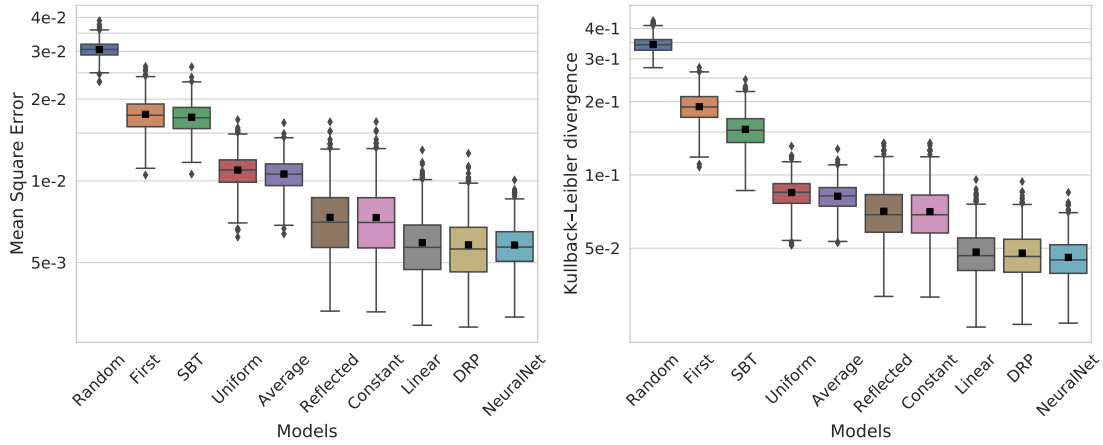


Fig. 5. Comparison of all models: Mean squared error (MSE) and Kullback–Leibler (KL) divergence of single-round influence matrix prediction for baseline algorithms and the proposed models. Evaluations are applied on 1000 bootstraps of the holdout test dataset (20% of the entire data). All models have access to the expertise and previous influence matrix for every team. The box shows the interquartile range of the errors, the whisker shows minimum and maximum of the range of the distribution, and the dots show the outliers. Baseline models: *Random* baseline is a randomly generated row-stochastic matrix. *First* predicts a team’s first influence matrix to be unchanged. *SBT* baseline uses the generalized Structural Balance Theory (81). *Uniform* predicts a matrix with all elements as $\frac{1}{n}$. *Average* predicts a team’s row-stochastic average influence matrix to be the most accurate prediction for any influence matrix. *Reflected* baseline uses reflected appraisal mechanism for prediction (31). *Constant* predicts the influence matrix to be unchanged from last measured one. Proposed models: Cognitive model based on Differentiation, Reversion, Perceived expertise model *DRP* takes into account the aforementioned hypotheses (1, 2, 3) to predict influence matrices. Moreover, Linear model using convex optimization (*Linear*) and Neural Networks model (*NeuralNet*) are proposed to learn important features from the logs to estimate influence matrices. The figure depicts the proposed models outperform baselines. Surprisingly, this figure shows the reflected appraisal model does not surpass the baseline of considering previous influence matrix to be unchanged (Constant model). This figure also shows that the cognitive model works competitively with the learning models showing the power behind our empirically proven hypotheses.

compared to all baselines with the neural network-based model surpassing all other models. The problem formulation for MSE of influence matrices is provided in Eq. [13], and for probability distribution estimation in every row of influence matrices is given in Eq. [14] (see Methods and Materials).

Table 3 sheds light on the importance of every feature set in the linear model optimized using convex optimization which was trained with 80% of the data. This table shows entry-wise l_1 -norm of estimated parameters in Eq. [13]. The values in table 3 are sorted from most to least important top to bottom. This result shows the previous influence matrix is the most important feature used to predict the next influence matrix. Interestingly, it also shows expertise is the second most of predictive power and text embedding is third. It shows sentiment, emotion, and quick responsiveness (response network) network are far less substantial in the estimation. It is worth mentioning that due to the origin of memory questions, there is only a brief chat happening for many of the members since they simply do not know the answer. That is probably the reason that text embedding is not as important as the correct answer rate.

Discussion

Interpersonal appraisal networks can be modeled as an influence matrix, where weighted edges signify positive or negative appraisals among people. Being able to estimate these influence matrices has important applications such as marketing advertisements, creating successful political campaigns, and improving the efficiency of communication among team members. The problem of influence matrix estimation has been studied previously either with simulated data or with a focus on estimating the total amount of influence from websites rather than estimating interpersonal influence within groups.

We collected data from human subjects answering trivia questions in teams of four. After individually answering a

Table 3. Importance features in predicting influence: Entry-wise l_1 -norm of estimated parameter matrix in linear model given in Eq. [13] which is trained with 80% of the data. This table shows the importance of each features in the proposed linear model. The embeddings (79), sentiments, and emotions all are computed from the message text content; however, responsiveness is computed from the timestamps of the messages.

	l_1 -norm of estimated parameters
Previous influence matrix	0.2137 ± 0.0027
Expertise	0.0239 ± 0.0027
Message content embedding	0.0111 ± 0.0003
Message sentiment	0.0078 ± 0.0010
Message emotion	0.0050 ± 0.0007
Message responsiveness	0.0041 ± 0.0004

question, they then collaborated to agree on a final answer through a chat system. The participants were periodically asked to assess their appraisals of each other. We built a machine learning-based model using text content, the time of messages, and individual task performance to estimate the collective influence matrix. We sought to find underlying factors that contribute to the accorded influence. We proposed a dynamical cognitive model, a linear model using convex optimization, and a neural network model alongside baselines from dynamical models and sociology literature to test our hypotheses. From these findings, we concluded that task performance and higher values of confidence were the two most salient factors in determining the amount of influence one receives in collaborative group settings. We believe this study on estimating underlying influence systems in a collaborative environment will spur the establishment of connections with a variety of fields and advance an interdisciplinary understanding of the design of social experiments.

Materials and Methods

In this section, we provide mathematical formulation regarding how the proposed dynamical model, linear, and deep neural network model alongside baselines efficiently frame and solve the influence matrix estimation problem. The proofs for all lemmas are provided in the Supplementary Information (SI).

Proposed cognitive dynamical models. We propose various discrete time dynamical models that characterize the evolution of the influence network based on various sociological concepts. Let the simplex be defined as $\Delta_n = \{x \in \mathbb{R}_{\geq 0}^n \mid \mathbf{1}_n^\top x = 1\}$. Given an estimate of a previous row-stochastic influence matrix $\hat{M}^{(t)}$ and an estimate of normalized or perceived expertise $x^{(t)} \in \Delta_n$, our models are in the general form

$$\hat{M}^{(t+1)} = T(\hat{M}^{(t)}, x^{(t)}) \quad \text{for } t \geq 1,$$

where $\hat{M}^{(t)}$ denote the influence matrix estimate at round t . Let $\hat{M}_d^{(t)} = [\hat{M}_{11}^{(t)}, \dots, \hat{M}_{nn}^{(t)}]^\top$ denote the vector of self-influence weights. Consider the normalized expertise and perceived expertise, defined as follows. *Normalized expertise* $\bar{y}^{(t)} \in \Delta_n$ is defined as

$$\bar{y}^{(t)} = (\mathbf{1}_n^\top y^{(t)})^{-1} y^{(t)} \quad [8]$$

and *perceived expertise* $\hat{y}^{(t)}(y^{(t)}, \hat{M}_d^{(t)}) \in \Delta_n$ is defined as

$$\hat{y}^{(t)}(y^{(t)}, \hat{M}_d^{(t)}) = (\hat{M}_d^{(t)\top} y^{(t)})^{-1} \text{diag}(\hat{M}_d^{(t)}) y^{(t)}. \quad [9]$$

Then depending on the model, $x^{(t)}$ is equal to either $\bar{y}^{(t)}$ or $\hat{y}^{(t)}$. Our proposed models use also a scaling parameter $\tau \in (0, 1)$ that can be adjusted to change the time-scale of the dynamics. If we have information on past reported influence matrices and expertise levels of team members, these models can be used to predict future influence matrices.

- *Differentiation model (D model):* Motivated by Hypothesis 1, this model assumes individuals assign influence based on the normalized, cumulative expertise [8], where individuals who perform better are accorded higher influence. The model is defined for all $i, j \in \{1, \dots, n\}$ as

$$\hat{M}_{ij}^{(t+1)} = (1 - \tau)\hat{M}_{ij}^{(t)} + \tau\bar{y}_j^{(t)}, \quad [10]$$

which reads in matrix form as $\hat{M}^{(t+1)} = (1 - \tau)\hat{M}^{(t)} + \tau\mathbf{1}_n\bar{y}^{(t)\top}$.

- *Differentiation, Reversion model (DR model):* Motivated by Hypotheses 1 and 2, this model is based on the D model and assumes high-performing individuals are accorded more influence and low-performing individuals tend to assign influence weights uniformly amongst team members. The model uses the normalized expertise [8] and is defined for all $i, j \in \{1, \dots, n\}$ as

$$\hat{M}_{ij}^{(t+1)} = (1 - \tau)\hat{M}_{ij}^{(t)} + \tau\left(\bar{y}_i^{(t)}\bar{y}_j^{(t)} + (1 - \bar{y}_i^{(t)})\frac{1}{n}\right), \quad [11]$$

which reads in matrix form as

$$\hat{M}^{(t+1)} = (1 - \tau)\hat{M}^{(t)} + \tau\left(\bar{y}^{(t)}\bar{y}^{(t)\top} + \frac{1}{n}(\mathbf{1}_n - \bar{y}^{(t)})\mathbf{1}_n^\top\right).$$

- **Cognitive model based on Differentiation, Reversion, Perceived expertise model (DRP model):** Motivated by Hypotheses 1, 2 and 3, this model is an extension of [12], where everyone's expertise is miscalculated based on their own self-confidence. The model then uses the perceived expertise [9] to learn how much influence is accorded to one another. Fig. 3 depicts for both single-round and multi-round prediction, using all three hypotheses baked in this model provides the most accurate and consistent estimation. This model is defined for all $i, j \in \{1, \dots, n\}$ as

$$\hat{M}_{ij}^{(t+1)} = (1 - \tau)\hat{M}_{ij}^{(t)} + \tau\left(\hat{y}_i^{(t)}\hat{y}_j^{(t)} + (1 - \hat{y}_i^{(t)})\frac{1}{n}\right). \quad [12]$$

The following Lemma states that the D, DR, and DRP model are well-posed and the dynamics preserves row-stochasticity of the influence matrices.

Lemma 1 (Dynamic models preserve row-stochasticity). *Consider the D model Eq. [10], DR model Eq. [11], and DRP model Eq. [12] with $\tau \in (0, 1)$ and $y^{(t)} = y = [0, 1]^n$. If $\hat{M}^{(1)}$ is row-stochastic, then $\hat{M}^{(t)}$ remains row-stochastic for all $t \geq 1$ under the D and DR model.*

If additionally, there exists at least one i such that $\hat{M}_{ii}^{(1)} > 0$ and $y_i > 0$, then the DRP model is well-posed for finite t and $\hat{M}^{(t)}$ remains row-stochastic for all $t \geq 1$.

Given constant expertise y , it is clear that the affine models, D and DR, converge. In simulations (see Supplementary Fig. S1), we also observe that the DRP model exhibits convergence behaviors to a unique equilibrium. The next Lemma illustrates convergence of the DRP model for $y = c\mathbf{1}_n$ with $c > 0$.

Lemma 2 (Equilibrium and convergence of DRP model with uniform expertise). *Consider the DRP model [12]. Assume for $\tau \in (0, 1)$, constant uniform expertise values $y^{(t)} = c\mathbf{1}_n$ with $c > 0$, $\hat{M}^{(1)}$ row-stochastic, and that there exists at least one i such that $\hat{M}_{ii}^{(1)} > 0$. Then $\lim_{t \rightarrow \infty} \hat{M}^{(t)} = \frac{1}{n}\mathbf{1}_n\mathbf{1}_n^\top$.*

The proofs for these lemmas can be found in the SI.

Proposed linear model. Using machine learning models we can take advantage of all available data to estimate influence matrices. Combining text, connectivity network, expertise, and historical appraisals produce a multi-dimensional prediction model. We have N teams of n individuals that go through T game rounds. To have a general format, we represent influence matrix for team m at round t by $M^{(m,t)}$. We represent all aforementioned features in matrix format (shown by $X_k^{(m,t)}$ for matrix feature k of team m at round t). We need to estimate the weight variables that maps the features to the influence matrix. In total, we assume there are K matrix variables, shown as W_k ; $k = 1$ to K . Ergo, a convex objective function for estimating the influence matrix is defined as

$$\min_{W_k: k=1 \text{ to } K, B} \sum_{m=1}^N \sum_{t=1}^T \left\| \sum_{k=1}^K X_k^{(m,t)} W_k^T + B - M^{(m,t)} \right\|_F^2 + \lambda \left(\sum_{k=1}^K \|W_k\|_{1,1} + \|B\|_{1,1} \right), \quad [13]$$

$$\text{Subject to } \sum_{m=1}^N \sum_{t=1}^T \sum_{k=1}^K X_k^{(m,t)} W_k^T + B \geq 0,$$

$$\mathbf{1}_n^T \left(\sum_{m=1}^N \sum_{t=1}^T \sum_{k=1}^K X_k^{(m,t)} W_k^T + B \right) = \mathbf{1}_n^T.$$

where $M^{(m,t)}$ is the ground truth influence matrix, self-reported by team m at round t . Depending on the application, for the history of the influence matrix, we may use only the first matrix, the average of all previous ones, or only the previous matrix. Variables to be calculated via optimization are the $n \times n$ weight matrices W_k . B is the $n \times n$ bias matrix also to be estimated. We also use an $l1$ -norm regularization to introduce sparsity to the estimated parameters that is commonly used in many real applications and also decrease the potential search space and therefore provides efficiency for the optimization solver.

Lemma 3. *The problem in Eq. [13] is convex.*

Based on the application, when only the probability distribution and the order of influence toward others is more important than exact values, we use cross-entropy as the loss function and KL divergence as the metric. In such a case, we can formulate the matrix estimation problem as the estimation of each row, which is a discrete distribution comprised of four numbers. Cross-entropy for two probability distribution of p and q is defined as $H(p, q) = -\sum_{i=1}^n p_i \log q_i$. In this study, the two probabilities are

$$p = M_{i,\cdot}, \quad \forall i \in [1, n]$$

$$q = \hat{M}_{i,\cdot} = \sigma(O_{i,\cdot}) = \sigma(W^T X_{i,\cdot} + b) \quad \forall i \in [1, n]$$

where σ represents Softmax function, $M_{i,\cdot}$ shows row i of matrix M , and W and b show the weight and bias variables to be estimated.

Lemma 4. *The optimization problem using the cross-entropy loss function on corresponding rows of two matrices M and \hat{M} can be written as*

$$\min_{W,b} - \sum_{m=1}^N \sum_{t=1}^T \sum_{j=1}^n \sum_{k=1}^n M_{j,k}^{(m,t)} \left(X_{j,k}^{(m,t)} W_{k,j} + b_j \right) - \log \sum_{l=1}^n \exp \left(X_{j,k}^{(m,t)} W_{k,j} + b_j \right) + \lambda \left(\|W\|_1 + \|b\|_1 \right) \quad [14]$$

The problem in Eq. [14] does not require any constraints to solve the convex optimization. First, because the Softmax function (σ) in this equation provides a discrete distribution in the format of vectors (all fall into $[0, 1]$ and sum up to 1). Second, since here we format the data points as vectors and not as matrices.

Lemma 5. *The problem in Eq. [14] is convex.*

The proofs for all these lemmas can be found in the SI.

Proposed deep neural network-based model. We can also learn the mapping defined by the three weight matrices as deep encoders in a two-tower model (82). In this regard, we apply end-to-end models to estimate the social influence matrices using multi-layered encoders from raw features to an influence matrix. This is described in Fig. 6. Each encoder is comprised of three fully connected Exponential Linear Unit (ELU) (83) layers, initialized by He *et al.* (84) Normal initialization, such that it draws samples from a truncated normal distribution centered on 0 with a standard deviation of $\sqrt{\frac{2}{f}}$ where f is the number of input units in the weight tensor. We use Dropout (85) after each fully connected layer to decrease overfitting. Then, all three outputs are concatenated and fed to another three fully connected layers with the same activation function to decrease the dimensionality of embedding vectors to an $n \times n$ matrix $M^{(m,t)}$, n being the number of individuals. Finally, cosine similarity of the two matrices $M^{(m,t)}$ and $\hat{M}^{(m,t)}$ is computed and the error is back-propagated using stochastic gradient descent.

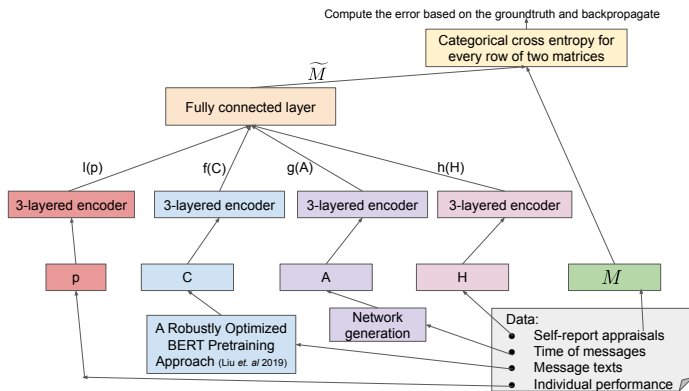


Fig. 6. Deep learning model architecture: A deep encoder model in a two-tower framework (82) for learning the three mappings of connectivity network, content of messages, and history of appraisals. The final layer computes the cosine similarity with the ground truth influence matrix and back-propagates the error using Stochastic Gradient Descent (SGD).

The deep method description is shown in Fig. 6. In this figure, the weights matrices in Eq. [13] are framed as a layers of deep neural networks. This model creates a non-convex problem; however, arguably with the abundance of data, a more effective model.

Baseline dynamical models.

• *Constant appraisal model:* This is a basic model which assumes the influence matrix remains constant over time. The model reads in matrix form as $\hat{M}^{(t+1)} = M^{(t)}$, or defined element-wise, for all $i, j \in \{1, \dots, n\}$ as

$$\hat{M}_{ij}^{(t+1)} = \hat{M}_{ij}^{(t)}. \quad [15]$$

• *Reflected appraisal model:* The reflected appraisal model is based on the model proposed in Mei *et al.* (31). The self-influence estimate $\hat{M}_{ii}^{(t+1)}$ increases relative to $\hat{M}_{ii}^{(t)}$ if the expertise of individual i , $y_i^{(t)}$, is larger than average team expertise observed by individual i , $\sum_{k=1}^n \hat{M}_{ik}^{(t)} y_k^{(t)}$. If $\hat{M}_{ii}^{(t)}$ increases, then the interpersonal weights $\hat{M}_{ij}^{(t+1)}$ for all $j \neq i$ are decreased so that $\hat{M}^{(t+1)}$ remains row-stochastic. The reflected appraisal model is defined element-wise for all $i, j \in \{1, \dots, n\}$ and $t > 0$ as

$$\hat{M}_{ii}^{(t+1)} = \hat{M}_{ii}^{(t)} + \hat{M}_{ii}^{(t)} \left(1 - \hat{M}_{ii}^{(t)} \right) \left(\bar{y}_i^{(t)} - \sum_{k=1}^n \hat{M}_{ik}^{(t)} \bar{y}_k^{(t)} \right), \quad [16]$$

$$\hat{M}_{ij}^{(t+1)} = \hat{M}_{ij}^{(t)} - \hat{M}_{ii}^{(t)} \hat{M}_{ij}^{(t)} \left(\bar{y}_i^{(t)} - \sum_{k=1}^n \hat{M}_{ik}^{(t)} \bar{y}_k^{(t)} \right),$$

which reads in matrix form as

$$\hat{M}^{(t+1)} = \hat{M}^{(t)} + \text{diag} \left((I_n - \hat{M}^{(t)}) \bar{y}^{(t)} \right) \text{diag}(\hat{M}_d^{(t)}) (I_n - \hat{M}^{(t)}).$$

• *Structural balance theory:* Structural balance theory is a long-established theory describing the dynamics that govern the sentiment of interpersonal relationships. Researchers have consistently delivered various theoretical (25–28) and empirical support (29, 30, 86) for the emergence of this phenomenon in myriad settings. In this study, we use a generalized Structural balance theory model (SBT) that is inspired by earlier research Kulakowski *et al.* (81). It predicts the dynamic of influence as introduced in the following

$$\hat{M}_{ij}^{(t+1)} = \frac{1}{n-2} \sum_{k=1, \text{ when } k \neq i, k \neq j}^n \hat{M}_{ik}^{(t)} \hat{M}_{kj}^{(t)}. \quad [17]$$

Code Availability

The source code is publicly available under https://github.com/omid55/appraisal_network_dynamics.

ACKNOWLEDGMENTS.

This work is supported by a UC Multicampus-National Lab Collaborative Research and Training (UC-NL-CRT) grant, titled “Political Conflict and Stability in Dynamic Networks,” under grant number LFR-18-547591, and by the U. S. Army Research Laboratory and U. S. Army Research Office under grant number W911NF-15-1-0577. We thank Dr. Fabio Fagnani and Dr. Giacomo Como for their invaluable discussions with authors regarding the dynamical cognitive models.

References

- MH DeGroot, Reaching a consensus. *J. Am. Stat. Assoc.* **69**, 118–121 (1974).
- NE Friedkin, EC Johnsen, Social influence and opinions. *J. Math. Sociol.* **15**, 193–206 (1990).
- A Das, S Gollapudi, K Munagala, Modeling opinion dynamics in social networks in *Proceedings of the 7th ACM International Conference on Web Search and Data Mining*. pp. 403–412 (2014).
- NE Friedkin, F Bullo, How truth wins in opinion dynamics along issue sequences. *Proc. Natl. Acad. Sci.* **114**, 11380–11385 (2017).
- P Jia, A MirTabatabaei, NE Friedkin, F Bullo, Opinion dynamics and the evolution of social power in influence networks. *SIAM Rev.* **57**, 367–397 (2015).
- C Ravazzi, R Tempo, F Dabbene, Learning influence structure in sparse social networks. *IEEE Transactions on Control. Netw. Syst.* **5**, 1976–1986 (2017).
- X Zheng, D Zeng, FY Wang, Social balance in signed networks. *Inf. Syst. Front.* **17**, 1077–1095 (2015).
- MH DeGroot, Reaching a consensus. *J. Am. Stat. Assoc.* **69**, 118–121 (1974).
- C Altafini, Consensus problems on networks with antagonistic interactions. *IEEE Transactions on Autom. Control.* **58**, 935–946 (2012).
- AV Proskurnikov, R Tempo, A tutorial on modeling and analysis of dynamic social networks. Part I. *Annu. Rev. Control.* **43**, 65–79 (2017).

11. W Chen, Y Wang, S Yang, Efficient influence maximization in social networks in *Proceedings of the 15th ACM SIGKDD International Conference on Knowledge Discovery and Data Mining*. pp. 199–208 (2009).
12. O Askarisichani, M Jalili, Influence maximization of informed agents in social networks. *Appl. Math. Comput.* **254**, 229–239 (2015).
13. J Leskovec, LA Adamic, BA Huberman, The dynamics of viral marketing. *ACM Transactions on Web* **1**, 5 (2007).
14. W Chen, C Wang, Y Wang, Scalable influence maximization for prevalent viral marketing in large-scale social networks in *Proceedings of the 16th ACM SIGKDD International Conference on Knowledge Discovery and Data Mining*. (ACM), pp. 1029–1038 (2010).
15. X Song, BL Tseng, CY Lin, MT Sun, Personalized recommendation driven by information flow in *Proceedings of the 29th Annual International ACM SIGIR Conference on Research and Development in Information Retrieval*. pp. 509–516 (2006).
16. D Ienco, F Bonchi, C Castillo, The meme ranking problem: Maximizing microblogging virality in *IEEE International Conference on Data Mining Workshops*. pp. 328–335 (2010).
17. Y Li, D Zhang, KL Tan, Real-time targeted influence maximization for online advertisements. *Proc. VLDB Endow.* **8**, 1070–1081 (2015).
18. J Weng, EP Lim, J Jiang, Q He, Twitterrank: finding topic-sensitive influential tweeters in *Proceedings of the third ACM International Conference on Web Search and Data Mining*. pp. 261–270 (2010).
19. E Bakshy, JM Hofman, WA Mason, DJ Watts, Everyone’s an influencer: quantifying influence on twitter in *Proceedings of the fourth ACM International Conference on Web Search and Data Mining*. pp. 65–74 (2011).
20. J Leskovec, et al., Cost-effective outbreak detection in networks in *Proceedings of the 13th ACM SIGKDD International Conference on Knowledge Discovery and Data Mining*. (ACM), pp. 420–429 (2007).
21. JRP French Jr., B Raven, The bases of social power in *Studies in Social Power*, ed. D Cartwright. (Institute for Social Research, University of Michigan), pp. 150–167 (1959).
22. EB Goldsmith, Social influence history and theories in *Social Influence and Sustainable Consumption*. (Springer), pp. 23–39 (2015).
23. NE Friedkin, A formal theory of reflected appraisals in the evolution of power. *Adm. Sci. Q.* **56**, 501–529 (2011).
24. P Jia, NE Friedkin, F Bullo, The coevolution of appraisal and influence networks leads to structural balance. *IEEE Transactions on Netw. Sci. Eng.* **3**, 286–298 (2016).
25. F Heider, Attitudes and cognitive organization. *The J. psychology* **21**, 107–112 (1946).
26. SA Marvel, J Kleinberg, RD Kleinberg, SH Strogatz, Continuous-time model of structural balance. *Proc. Natl. Acad. Sci.* **108**, 1771–1776 (2011).
27. A Srinivasan, Local balancing influences global structure in social networks. *Proc. Natl. Acad. Sci.* **108**, 1751–1752 (2011).
28. G Facchetti, G Iacono, C Altafini, Computing global structural balance in large-scale signed social networks. *Proc. Natl. Acad. Sci.* **108**, 20953–20958 (2011).
29. M Szell, R Lambiotte, S Thurner, Multirelational organization of large-scale social networks in an online world. *Proc. Natl. Acad. Sci.* **107**, 13636–13641 (2010).
30. O Askarisichani, et al., Structural balance emerges and explains performance in risky decision-making. *Nat. Commun.* **10**, 2648 (2019).
31. W Mei, NE Friedkin, K Lewis, F Bullo, Dynamic models of appraisal networks explaining collective learning. *IEEE Transactions on Autom. Control.* **63**, 2898–2912 (2017).
32. JR Austin, Transactive memory in organizational groups: the effects of content, consensus, specialization, and accuracy on group performance. *J. Appl. Psychol.* **88**, 866 (2003).
33. K Lewis, Measuring transactive memory systems in the field: scale development and validation. *J. Appl. Psychol.* **88**, 587 (2003).
34. K Lewis, Knowledge and performance in knowledge-worker teams: A longitudinal study of transactive memory systems. *Manag. Sci.* **50**, 1519–1533 (2004).
35. K Lewis, D Lange, L Gillis, Transactive memory systems, learning, and learning transfer. *Organ. Sci.* **16**, 581–598 (2005).
36. YC Yuan, I Carboni, K Ehrlich, The impact of awareness and accessibility on expertise retrieval: A multilevel network perspective. *J. Am. Soc. for Inf. Sci. Technol.* **61**, 700–714 (2010).
37. DW Liang, R Moreland, L Argote, Group versus individual training and group performance: The mediating role of transactive memory. *Pers. Soc. Psychol. Bull.* **21**, 384–393 (1995).
38. PR Laughlin, AL Ellis, Demonstrability and social combination processes on mathematical intellectual tasks. *J. Exp. Soc. Psychol.* **22**, 177–189 (1986).
39. PR Laughlin, Social combination processes of cooperative problem-solving groups on verbal intellectual tasks. *Prog. Soc. Psychol.* **1**, 127–155 (1980).
40. JV Wood, Theory and research concerning social comparisons of personal attributes. *Psychol. Bull.* **106**, 231 (1989).
41. JA Shepperd, Productivity loss in performance groups: A motivation analysis. *Psychol. bulletin* **113**, 67 (1993).
42. JA Shepperd, RA Wright, Individual contributions to a collective effort: An incentive analysis. *Pers. social psychology bulletin* **15**, 141–149 (1989).
43. JR Beatty, RW Haas, D Sciglimpaglia, Using peer evaluations to assess individual performances in group class projects. *J. Mark. Educ.* **18**, 17–27 (1996).
44. HK Davison, V Mishra, MN Bing, DD Frink, How individual performance affects variability of peer evaluations in classroom teams: A distributive justice perspective. *J. Manag. Educ.* **38**, 43–85 (2014).
45. JA Drexler Jr, TA Beehr, TA Stetz, Peer appraisals: Differentiation of individual performance on group tasks. *Hum. Resour. Manag. Publ. Coop. with Sch. Bus. Adm. The Univ. Mich. alliance with Soc. Hum. Resour. Manag.* **40**, 333–345 (2001).
46. JS Miller, RL Cardy, Self-monitoring and performance appraisal: rating outcomes in project teams. *J. Organ. Behav. The Int. J. Ind. Occup. Organ. Psychol. Behav.* **21**, 609–626 (2000).
47. JP Thomas, RG McFadyen, The confidence heuristic: A game-theoretic analysis. *J. Econ. Psychol.* **16**, 97–113 (1995).
48. PC Price, ER Stone, Intuitive evaluation of likelihood judgment producers: Evidence for a confidence heuristic. *J. Behav. Decis. Mak.* **17**, 39–57 (2004).
49. H London, PJ Meldman, A VAN C. LANCKTON, The jury method: How the persuader persuades. *Public Opin. Q.* **34**, 171–183 (1970).
50. O Askarisichani, M Jalili, Inference of hidden social power through opinion formation in complex networks. *IEEE Transactions on Netw. Sci. Eng.* **4**, 154–164 (2017).
51. LE Castro, NI Shaikh, A particle-learning-based approach to estimate the influence matrix of online social networks. *Comput. Stat. & Data Analysis* **126**, 1–18 (2018).
52. LE Castro, NI Shaikh, Influence estimation and opinion-tracking over online social networks. *Int. J. Bus. Anal.* **5**, 24–42 (2018).
53. ST Smith, EK Kao, DC Shah, O Simek, DB Rubin, Influence estimation on social media networks using causal inference in *IEEE Statistical Signal Processing Workshop (SSP)*. pp. 328–332 (2018).
54. M Gomez-Rodriguez, L Song, N Du, H Zha, B Schölkopf, Influence estimation and maximization in continuous-time diffusion networks. *ACM Transactions on Inf. Syst.* **34**, 1–33 (2016).
55. N Du, L Song, MG Rodriguez, H Zha, Scalable influence estimation in continuous-time diffusion networks in *Advances in Neural Information Processing Systems*. pp. 3147–3155 (2013).
56. Q Deng, Y Dai, How your friends influence you: Quantifying pairwise influences on twitter in *International Conference on Cloud and Service Computing*. (IEEE), pp. 185–192 (2012).
57. S Ye, SF Wu, Measuring message propagation and social influence on twitter.com in *International Conference on Social Informatics*. (Springer), pp. 216–231 (2010).
58. F Riquelme, P González-Cantergiani, Measuring user influence on twitter: A survey. *Inf. Process. & Manag.* **52**, 949–975 (2016).
59. A Almaatouq, et al., Adaptive social networks promote the wisdom of crowds. *Proc. Natl. Acad. Sci.* **117**, 11379–11386 (2020).
60. C Manteli, B Van Den Hooff, H Van Vliet, The effect of governance on global software development: An empirical research in transactive memory systems. *Inf. Softw. Technol.* **56**, 1309–1321 (2014).
61. CC Huang, PK Chen, Exploring the antecedents and consequences of the transactive memory system: An empirical analysis. *J. Knowl. Manag.* **22**, 92–118 (2018).
62. P Bonacich, Power and centrality: A family of measures. *Am. J. Sociol.* **92**, 1170–1182 (1987).
63. TN Wisdom, X Song, RL Goldstone, Social learning strategies in networked groups. *Cogn. science* **37**, 1383–1425 (2013).
64. R Boyd, PJ Richerson, J Henrich, The cultural niche: Why social learning is essential for human adaptation. *Proc. Natl. Acad. Sci.* **108**, 10918–10925 (2011).
65. J Becker, D Brackbill, D Centola, Network dynamics of social influence in the wisdom of crowds. *Proc. Natl. Acad. Sci.* **114**, E5070–E5076 (2017).
66. G Madirolas, GG de Polavieja, Improving collective estimations using resistance to social influence. *PLoS Comput. Biol.* **11**, e1004594 (2015).
67. BD Pulford, AM Colman, EK Buabang, EM Krockow, The persuasive power of knowledge: Testing the confidence heuristic. *J. Exp. Psychol. Gen.* **147**, 1431 (2018).
68. H Mercier, D Sperber, “two heads are better” stands to reason. *Science* **336**, 979–979 (2012).
69. R Hertwig, Tapping into the wisdom of the crowd—with confidence. *Science* **336**, 303–304 (2012).
70. B Everitt, A Skronal, *The Cambridge dictionary of statistics*. (Cambridge University Press Cambridge) Vol. 106, (2002).
71. CW Granger, Investigating causal relations by econometric models and cross-spectral methods. *Econom. J. Econom. Soc.* **37**, 424–438 (1969).
72. CW Granger, Testing for causality: a personal viewpoint. *J. Econ. Dyn. Control.* **2**, 329–352 (1980).
73. CW Granger, *Essays in econometrics: collected papers of Clive WJ Granger*. (Cambridge University Press) Vol. 32, (2001).
74. Y Benjamini, Y Hochberg, Controlling the false discovery rate: a practical and powerful approach to multiple testing. *J. Royal Stat. Soc. Ser. B (Methodological)* **57**, 289–300 (1995).
75. V Amelkin, O Askarisichani, YJ Kim, TW Malone, AK Singh, Dynamics of collective performance in collaboration networks. *PLoS One* **13**, e0204547 (2018).
76. CJ Hutto, E Gilbert, Vader: A parsimonious rule-based model for sentiment analysis of social media text in *Eighth International AAAI Conference on weblogs and social media*. (2014).
77. MM Bradley, PJ Lang, Affective norms for english words (anew): Instruction manual and affective ratings, (Technical report C-1, the center for research in psychophysiology . . .), Technical report (1999).
78. D Cer, et al., Universal sentence encoder. *ArXiv preprint arXiv:1803.11175 [cs]* (2018).
79. Y Liu, et al., Roberta: A robustly optimized bert pretraining approach. *arXiv preprint arXiv:1907.11692 [cs]* (2019).
80. J Devlin, MW Chang, K Lee, K Toutanova, Bert: Pre-training of deep bidirectional transformers for language understanding. *arXiv preprint arXiv:1810.04805 [cs]* (2018).
81. K Kulakowski, P Gawroński, P Groniek, The heider balance: A continuous approach. *Int. J. Mod. Phys. C* **16**, 707–716 (2005).
82. X He, et al., Neural collaborative filtering in *Proceedings of the 26th International Conference on World Wide Web*. (International World Wide Web Conferences Steering Committee), pp. 173–182 (2017).
83. DA Clevert, T Unterthiner, S Hochreiter, Fast and accurate deep network learning by exponential linear units (elus). *arXiv preprint arXiv:1511.07289 [cs]* (2015).
84. K He, X Zhang, S Ren, J Sun, Delving deep into rectifiers: Surpassing human-level performance on imagenet classification in *Proceedings of the IEEE International Conference on Computer Vision*. pp. 1026–1034 (2015).
85. N Srivastava, G Hinton, A Krizhevsky, I Sutskever, R Salakhutdinov, Dropout: a simple way to prevent neural networks from overfitting. *J. Mach. Learn. Res.* **15**, 1929–1958 (2014).
86. NE Friedkin, AV Proskurnikov, F Bullo, Positive contagion and the macrostructures of generalized balance. *Netw. Sci.* **7**, 445–458 (2019).
87. S Boyd, L Vandenberghe, *Convex optimization*. (Cambridge university press), (2004).
88. S Diamond, S Boyd, CVXPY: A Python-embedded modeling language for convex optimization. *J. Mach. Learn. Res.* **17**, 1–5 (2016).
89. NE Friedkin, EC Johnsen, Social influence and opinions. *J. Math. Sociol.* **15**, 193–206 (1990).

Supplementary Information for Expertise and confidence explain how social influence evolves along intellectual tasks

1. Methods

In this section, we provide remarks on the cognitive dynamical model and rigorous proofs for every lemma introduced in the main paper.

A. Auxiliary remarks for the cognitive dynamical model.

As defined in the main text, the Differentiation, Reversion, Perceived expertise (DRP) model is written in matrix form as

$$\hat{M}^{(t+1)} = (1 - \tau)\hat{M}^{(t)} + \tau \left(\hat{y}^{(t)} \hat{y}^{(t)\top} + \frac{1}{n} (\mathbb{1}_n - \hat{y}^{(t)}) \mathbb{1}_n^\top \right), \quad [18]$$

where $\hat{M}_d^{(t)} = [\hat{M}_{11}^{(t)}, \dots, \hat{M}_{nn}^{(t)}]^\top \in [0, 1]^n$ denotes the vector of self-influence weights of the influence matrix at time $t \geq 1$ and $\hat{y}^{(t)} = (y^\top \hat{M}_d^{(t)})^{-1} \text{diag}(y) \hat{M}_d^{(t)} \in \Delta_n$ denotes the normalized perceived expertise.

For the DRP model, the dynamics of the self-influence matrix weights is closed from the dynamics of the interpersonal influence weights, and can be written as only a function of $\hat{M}_d^{(t)}$,

$$\hat{M}_d^{(t+1)} = (1 - \tau)\hat{M}_d^{(t)} + \tau \left(\text{diag}(\hat{y}^{(t)}) \hat{y}^{(t)} + \text{diag}(\mathbb{1}_n - \hat{y}^{(t)}) \frac{1}{n} \mathbb{1}_n \right). \quad [19]$$

Then the dynamics of the interpersonal influence evolve as a function of the self-influence weights and the initial condition $\hat{M}^{(1)}$. This cascading effect illustrates how confidence drives influence.

B. Proof of Lemma 1.

Per our assumption that there exists at least one i such that $\hat{M}_{ii}^{(1)} > 0$ and $y_i > 0$, then $y^\top \hat{M}_d^{(0)} > 0$. Additionally, the DRP model guarantees that $\hat{M}_{ij}^{(t)} \geq (1 - \tau)^{(t-1)} \hat{M}_{ij}^{(1)} \geq 0$ for all i, j and finite time $t \geq 2$.

Next we show that the DRP dynamics preserves row-stochasticity. By definition, the sum of the perceived expertise is $\mathbb{1}_n^\top \hat{y}^{(t)} = (y^\top \hat{M}_d^{(t)})^{-1} y^\top \hat{M}_d^{(t)} = 1$. Then, we have

$$\begin{aligned} \hat{M}^{(t+1)} \mathbb{1}_n &= (1 - \tau)\hat{M}^{(t)} \mathbb{1}_n + \tau \left(\hat{y}^{(t)} \hat{y}^{(t)\top} \mathbb{1}_n + \frac{1}{n} (\mathbb{1}_n - \hat{y}^{(t)}) \mathbb{1}_n^\top \mathbb{1}_n \right) \\ &= (1 - \tau)\mathbb{1}_n + \tau \left(\hat{y}^{(t)} + (\mathbb{1}_n - \hat{y}^{(t)}) \right) \\ &= (1 - \tau)\mathbb{1}_n + \tau \mathbb{1}_n = \mathbb{1}_n. \end{aligned}$$

Therefore, $\hat{M}^{(t)}$ remains row-stochastic and well-posed for finite time $t \geq 1$. □

C. Proof of Lemma 2.

Since the dynamics of $\hat{M}^{(t+1)}$ can be described as a function of $M_d^{(t)}$, then it is sufficient to prove convergence of the self-influence weights given by the dynamics [19]. Note that $\hat{y}^{(t)} = (y^\top \hat{M}_d^{(t)})^{-1} \text{diag}(y) \hat{M}_d^{(t)} = (cy^\top \hat{M}_d^{(t)})^{-1} \text{diag}(cy) \hat{M}_d^{(t)}$ for any $c > 0$. Then per our assumption that $y = c\mathbb{1}_n$, we can assume $y = \mathbb{1}_n$ without loss of generality and $\hat{y}^{(t)} = (\mathbb{1}_n^\top \hat{M}_d^{(t)})^{-1} \hat{M}_d^{(t)}$. For our proof, first, we show that all trajectories satisfying our initial condition assumptions reach the forward-invariant set $\Omega = \{\hat{M}_d^{(t)} \in [0, 1]^n \mid \mathbb{1}_n^\top \hat{M}_d^{(t)} \geq 1\}$. Second, we define a function $V : [0, 1]^n \rightarrow \mathbb{R}$ that we prove is a Lyapunov function for $\hat{M}_d^{(t)} \in \Omega$.

From the dynamics, all influence weight values become strictly positive for $t \geq 2$, regardless of the initial condition. If $\hat{M}_{ij}^{(1)} = 0$, then $\hat{M}_{ij}^{(2)} = \frac{\tau}{n}$ and if $\hat{M}_{ij}^{(1)} > 0$, then $\hat{M}_{ij}^{(2)} > (1 - \tau)\hat{M}_{ij}^{(1)}$.

Consider $\hat{M}_d^{(t)} \notin \Omega$ where $\mathbb{1}_n^\top \hat{M}_d^{(t)} < 1$, then

$$\mathbb{1}_n^\top \hat{M}_d^{(t+1)} = (1 - \tau)\mathbb{1}_n^\top \hat{M}_d^{(t)} + \tau \hat{y}^{(t)\top} \hat{y}^{(t)} + \tau - \frac{\tau}{n} > \mathbb{1}_n^\top \hat{M}_d^{(t)} - \tau + \frac{\tau}{n} + \tau - \frac{\tau}{n} = \mathbb{1}_n^\top \hat{M}_d^{(t)}.$$

The inequality from the last line follows from the fact that $\hat{y}^{(t)\top} \hat{y}^{(t)} \geq \frac{1}{n}$, which can be found by formulating the minimization problem of $\hat{y}^{(t)\top} \hat{y}^{(t)}$ as a constrained convex optimization problem and applying the KKT conditions. Therefore if $\hat{M}_d^{(t)} \notin \Omega$ and $\mathbb{1}_n^\top \hat{M}_d^{(t+1)} > \mathbb{1}_n^\top \hat{M}_d^{(t)}$, there exists some finite time $T > t$ such that $\hat{M}_d^{(T)} \in \Omega$. Next, consider $\hat{M}_d^{(t)} \in \Omega$ implies

$$\mathbb{1}_n^\top \hat{M}_d^{(t+1)} \geq (1 - \tau)\mathbb{1}_n^\top \hat{M}_d^{(t)} - \tau + \frac{\tau}{n} + \tau - \frac{\tau}{n} \geq 1.$$

Since the dynamics also preserves row-stochasticity of the influence network by Lemma 1, then $\mathbb{1}_n^\top \hat{M}_d^{(t)} \leq n$ and we have shown that Ω is a compact forward-invariant set, where trajectories that enter Ω remain in Ω .

Now we prove that all trajectories in Ω converge to the equilibrium $\hat{M}_d^{(*)}$. It is straightforward to verify that the equilibrium of Eq. [19] is $\hat{M}_d^{(*)} = \frac{1}{n} \mathbb{1}_n$, which corresponds to the influence network equilibrium $\hat{M}^{(*)} = \frac{1}{n} \mathbb{1}_n \mathbb{1}_n^\top$. We define $V(\hat{M}_d^{(t)})$ as

$$V(\hat{M}_d^{(t)}) = \max_{i \in \{1, \dots, n\}} \left\{ \hat{M}_{ii}^{(t)} - \frac{1}{n} \right\},$$

where $V(\frac{1}{n}\mathbb{1}_n) = 0$ and $V(\hat{M}_d^{(t)}) > 0$ for $\hat{M}_d^{(t)} \in \Omega \setminus \frac{1}{n}\mathbb{1}_n$. Next we show that $V(\hat{M}_d^{(t+1)}) < V(\hat{M}_d^{(t)})$ for $\hat{M}_d^{(t)} \in \Omega \setminus \frac{1}{n}\mathbb{1}_n$. Note that for $\hat{y}^{(t)} \in \Delta_n$ and $\hat{M}_d^{(t)} \in \Omega$, then $\hat{y}_i^{(t)} \leq \hat{M}_{ii}^{(t)}$ and $\max_i \{\hat{M}_{ii}^{(t)}\} \geq \frac{1}{n}$, which are used for the following bounds.

$$\begin{aligned} V(\hat{M}_d^{(t+1)}) - V(\hat{M}_d^{(t)}) &= \max_{i \in \{1, \dots, n\}} \left\{ \hat{M}_{ii}^{(t+1)} - \frac{1}{n} \right\} - \max_{i \in \{1, \dots, n\}} \left\{ \hat{M}_{ii}^{(t)} - \frac{1}{n} \right\} \\ &\leq (1 - \tau) \max_{i \in \{1, \dots, n\}} \left\{ \hat{M}_{ii}^{(t)} - \frac{1}{n} \right\} + \tau \max_{i \in \{1, \dots, n\}} \left\{ \hat{y}_i^{(t)} \left(\hat{y}_i^{(t)} - \frac{1}{n} \right) \right\} - \max_{i \in \{1, \dots, n\}} \left\{ \hat{M}_{ii}^{(t)} - \frac{1}{n} \right\} \\ &\leq -\tau \max_{i \in \{1, \dots, n\}} \left\{ \hat{M}_{ii}^{(t)} - \frac{1}{n} \right\} + \tau \hat{M}_{ii}^{(t)} \max_{i \in \{1, \dots, n\}} \left\{ \hat{M}_{ii}^{(t)} - \frac{1}{n} \right\} < 0. \end{aligned}$$

As a result, all trajectories reach Ω in finite time and trajectories in Ω approach $\lim_{t \rightarrow \infty} \max_i \{\hat{M}_{ii}^{(t)}\} = \frac{1}{n}$, which can only occur for $\hat{M}_d^{(*)} = \frac{1}{n}\mathbb{1}_n$. For $\hat{M}_d^{(t)} = \hat{M}_d^{(*)}$, the dynamics of the interpersonal influence weights simplify to a stable affine system,

$$\hat{M}_{ij}^{(t+1)} = (1 - \tau)\hat{M}_{ij}^{(t)} + \tau \left(\hat{y}_i^{(t)} \hat{y}_j^{(t)} + (1 - \hat{y}_i^{(t)}) \frac{1}{n} \right).$$

Therefore, for any $\hat{M}^{(1)} \in [0, 1]^{n \times n}$ with at least one strictly positive diagonal entry, then $\lim_{t \rightarrow \infty} \hat{M}^{(t)} = \frac{1}{n}\mathbb{1}_n^T \mathbb{1}_n$. \square

D. Proof of Lemma 3.

With respect to variables W_k for any $k = 1$ to K and B , the loss function $\sum_{m=1}^N \sum_{t=1}^T \left\| \sum_{k=1}^K X_k^{(m,t)} W_k^T + B - M^{(m,t)} \right\|_F^2$ is a summation of multiple squared Frobenius norms. The regularization term $\sum_{k=1}^K \|W_k\|_{1,1} + \|B\|_{1,1}$ is also a summation of $l1$ -norms. All of which are convex functions (87). Both constraints $\sum_{m=1}^N \sum_{t=1}^T \sum_{k=1}^K X_k^{(m,t)} W_k^T + B \geq 0$ and $\mathbb{1}_n^T \left(\sum_{m=1}^N \sum_{t=1}^T \sum_{k=1}^K X_k^{(m,t)} W_k^T + B \right) = \mathbb{1}_n^T$ are linear combination of variables and hence affine functions. To this end, all of the inequality constraints are convex, and all equality constraints are affine. Therefore, the problem is convex, it has a globally optimal solution, and we can solve this equation with a convex optimization solver, CVXPY (88). \square

E. Proof of Lemma 4.

The objective function using cross-entropy can be derived, step by step, as follows,

$$\begin{aligned} \text{loss} &= \sum_{m=1}^N \sum_{t=1}^T \sum_{j=1}^n H(M_{j,\cdot}^{(m,t)}, \hat{M}_{j,\cdot}^{(m,t)}) \\ &= \sum_{m=1}^N \sum_{t=1}^T \sum_{j=1}^n - \sum_{k=1}^n M_{j,k}^{(m,t)} \log \hat{M}_{j,k}^{(m,t)} \\ &= - \sum_{m=1}^N \sum_{t=1}^T \sum_{j=1}^n \sum_{k=1}^n M_{j,k}^{(m,t)} \log \sigma(O_{j,k}^{(m,t)}) \\ &= - \sum_{m=1}^N \sum_{t=1}^T \sum_{j=1}^n \sum_{k=1}^n M_{j,k}^{(m,t)} \log \frac{\exp(O_{j,k}^{(m,t)})}{\sum_{l=1}^n \exp(O_{j,l}^{(m,t)})} \\ &= - \sum_{m=1}^N \sum_{t=1}^T \sum_{j=1}^n \sum_{k=1}^n M_{j,k}^{(m,t)} \left(O_{j,k}^{(m,t)} - \log \sum_{l=1}^n \exp(O_{j,l}^{(m,t)}) \right) \\ &= - \sum_{m=1}^N \sum_{t=1}^T \sum_{j=1}^n \sum_{k=1}^n M_{j,k}^{(m,t)} \left(X_{j,k}^{(m,t)} W_{k,j} + b_j - \log \sum_{l=1}^n \exp(X_{j,k}^{(m,t)} W_{k,j} + b_j) \right). \end{aligned}$$

Therefore, it results to

$$\begin{aligned} \text{objective} &= \text{loss} + \lambda \left(\|W\|_1 + \|b\|_1 \right) \\ &= - \sum_{m=1}^N \sum_{t=1}^T \sum_{j=1}^n \sum_{k=1}^n M_{j,k}^{(m,t)} \left(X_{j,k}^{(m,t)} W_{k,j} + b_j - \log \sum_{l=1}^n \exp(X_{j,k}^{(m,t)} W_{k,j} + b_j) \right) + \lambda \left(\|W\|_1 + \|b\|_1 \right) \end{aligned}$$

The final equation for the objective function is the same as Eq. [14] from the main paper. \square

F. Proof of Lemma 5.

With respect to variables W, b , the problem is a summation of an affine function $(-X_{j,k}^{(m,t)} W_{k,j})$, log-sum-exp term $(\log \sum_{l=1}^n \exp(X_{j,k}^{(m,t)} W_{k,j} + b_j))$ and two $l1$ -norms regularization terms $(-\lambda(\|W\|_1 + \|b\|_1))$. It has been proved mathematically

that the expression $\log \sum \exp(r)$ for any real r is convex in R^n (87). In here, r is an affine function $-X_{j,k}^{(m,t)} W_{k,j}$ with respect to variables W, b . Hence, the problem is a summation of an affine and two convex terms which preserves convexity and produces a convex function (87). Therefore, the minimization problem is convex, it has a globally optimal solution, and we can solve this equation with the aforementioned convex optimization solver. \square

2. Results

Here we describe the simulation results for equilibrium of the proposed dynamical model. Fig. 7 illustrates how the self-influence weights of the DRP model [18] with constant expertise y and time scale $\tau = 0.4$ evolve over time. The interpersonal influence weights are not plotted, since they are a function of $\hat{M}^{(1)}, \hat{M}_d^{(t)}$, and y .

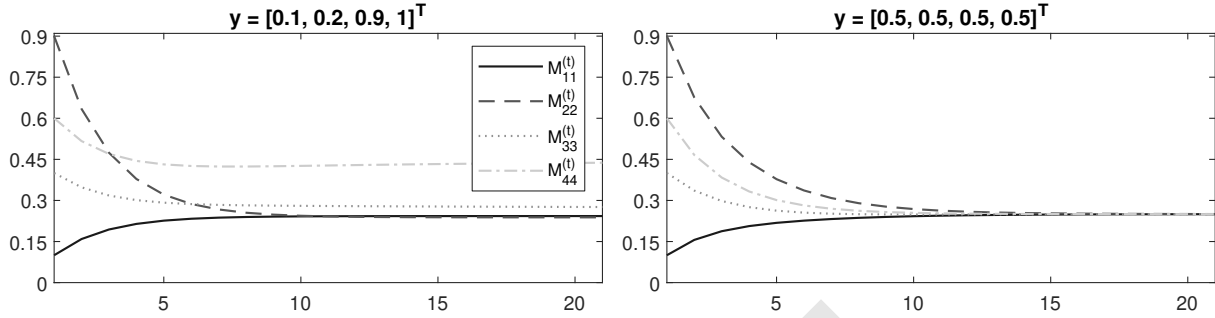


Fig. 7. For a team of 4 individuals, the plots depict the evolution of the self-influence matrix weights \hat{M}_{ii} for all $i \in \{1, \dots, 4\}$ obeying the DRP model [18] with constant expertise y as specified and time scale $\tau = 0.4$. In general, the self-influence overestimates low-performers and underestimates high-performers. However, when all individuals have the same expertise level, then $\hat{M}^{(t)}$ converges to $\frac{1}{n} \mathbf{1}_n \mathbf{1}_n^T$.

Fig. 8 demonstrates the Pearson correlations of every pair of metrics defined in Definitions. In this figure, all correlations are statistically significant as their corresponding p -values have been corrected using the Benjamini-Hochberg (BH) procedure (74) with False Discovery Rate of 5% has the required p -value < 0.018 as the statistical significance threshold. Note that global persuasiveness is the stationary probability of the influence matrix after removing its main diagonal (defined in Eq. [3]). This result shows that expertise is statistically correlated with the amount of appraisal one would receive by others in a team.



Fig. 8. Pearson correlation (r -value) of metrics on influence and expertise after answering all 45 questions with statistical significance of p -value < 0.018 . All metrics are formally presented in the main paper. The threshold for p -value is chosen using Benjamini-Hochberg (BH) procedure with False Discovery Rate of 5% (74). Persuasiveness for every subject in the final reported influence matrix vs. the expertise by the same subject has the coefficients r -value = 0.35 and p -value $< 2e-4$. This result shows that expertise is statistically correlated with the amount of appraisal one would receive by others in a team; this phenomenon is consistent with research on Transactive Memory System (TMS) (33–35). Surprisingly, this also shows in about two hours with indirect performance exposure, team members are still able to uncover each other's expertise. Moreover, confidence and appraise by others are also statistically correlated which is aligned with the research in confidence heuristics (47, 48).

For more details on the results shown in Fig. 4 from the main paper, we provide Table 6. Also for more details on the results shown in Fig. 5 from the main paper, we provide Table 4 and Table 5 to show MSE and KL divergence, respectively. All models use previous influence matrix and expertise. Similarly, neural network-based model surpasses all baselines and provides statistically and significantly lower error rate.

Table 4. MSE of estimated influence matrix from the ground truth in the test set of influence matrices reported by individuals. The number in parenthesis shows the standard error in 1000 bootstrap on test set. This table also depicts the proposed learning models (neural network-based and linear) outperform baselines. Surprisingly, it also shows the reflected appraisal does not surpass the baseline of considering previous influence matrix to be unchanged (constant baseline). Also interestingly, this table shows that the cognitive based on Differentiation, Reversion, Perceived (DRP) model Eq. [12] works competitively with the learning models showing the power behind this social phenomenon (89).

Features \ Models	Random baseline	First baseline	SBT baseline	Uniform baseline	Average baseline	Reflected appraisal model	Constant baseline	Linear model	Cognitive DRP-based model	Neural network-based model
previous influence matrix	0.0305 (0.00007)	0.0176 (0.00008)	0.0172 (0.00007)	0.0110 (0.00004)	0.0106 (0.00005)	N/A	0.0073 (0.00007)	0.0061 (0.00005)	N/A	0.0059 (0.00003)
previous influence matrix, expertise	0.0305 (0.00007)	0.0176 (0.00008)	0.0172 (0.00007)	0.0110 (0.00004)	0.0106 (0.00005)	0.0073 (0.00007)	0.0073 (0.00007)	0.0059 (0.00005)	0.0058 (0.00005)	0.0058 (0.00003)

Table 5. KL divergence of estimated influence matrix from the ground truth in the test set of influence matrices reported by individuals. The number in parenthesis shows the standard error in 1000 bootstrap on test set. Other designations in the table are the same as table 4.

Features \ Models	Random baseline	First baseline	SBT baseline	Uniform baseline	Average baseline	Reflected appraisal model	Constant baseline	Linear model	Cognitive DRP-based model	Neural network-based model
previous influence matrix	0.3431 (0.0008)	0.1908 (0.0009)	0.1540 (0.0008)	0.0818 (0.0003)	0.0709 (0.0006)	N/A	0.0707 (0.0006)	0.0494 (0.0003)	N/A	0.0479 (0.0003)
previous influence matrix, expertise	0.3431 (0.0008)	0.1908 (0.0009)	0.1540 (0.0008)	0.0818 (0.0003)	0.0709 (0.0006)	0.0709 (0.0006)	0.0707 (0.0006)	0.0482 (0.0003)	0.0478 (0.0003)	0.0459 (0.0003)

Table 6. Improvement in machine learning models by adding more features: Average of Mean Square Error (MSE) of estimated influence matrix from the ground truth in the test set of influence matrices reported by individuals. The number in parenthesis shows the standard error in 1000 bootstrap on test error.

Features \ Models	Random baseline	First baseline	Uniform baseline	Average baseline	Linear model	Neural Network-based model
expertise	0.0305 (0.00007)	0.0176 (0.00008)	0.0110 (0.00005)	0.0106 (0.00004)	0.0106 (0.00005)	0.0102 (0.00004)
expertise, first influence matrix	0.0305 (0.00007)	0.0176 (0.00008)	0.0110 (0.00005)	0.0106 (0.00004)	0.0093 (0.00005)	0.0079 (0.00003)
expertise, first influence matrix, response network	0.0305 (0.00007)	0.0176 (0.00008)	0.0110 (0.00005)	0.0106 (0.00004)	0.0093 (0.00005)	0.0072 (0.00003)
expertise, first influence matrix, response network, sentiment network, emotion network	0.0305 (0.00007)	0.0176 (0.00008)	0.0110 (0.00005)	0.0106 (0.00004)	0.0093 (0.00004)	0.0070 (0.00003)
expertise, first influence matrix, response network, sentiment network, emotion network, content embedding	0.0305 (0.00007)	0.0176 (0.00008)	0.0110 (0.00005)	0.0106 (0.00004)	0.0090 (0.00004)	0.0069 (0.00003)
expertise, first influence matrix, response network, sentiment network, emotion network, content embedding, average of previous influence matrices	0.0305 (0.00007)	0.0176 (0.00008)	0.0110 (0.00005)	0.0106 (0.00004)	0.0076 (0.00005)	0.0066 (0.00003)